

2025

Assessing adaptive capabilities in triple negative breast cancer cells

<https://hdl.handle.net/2144/52341>

"Downloaded from OpenBU. Boston University's institutional repository."

BOSTON UNIVERSITY

ARAM V. CHOBANIAN & EDWARD AVEDISIAN SCHOOL OF MEDICINE

Thesis

**ASSESSING ADAPTIVE CAPABILITIES
IN TRIPLE NEGATIVE BREAST CANCER CELLS**

By

VAN MIGUEL LEOSALA LAGASON

B.S., The Ohio State University, 2021

Submitted in partial fulfillment of the
requirements for the degree of

Master of Science

2025

© 2025 by
VAN MIGUEL LEOSALA LAGASON
All rights reserved

Approved by

First Reader

Hui Feng, MD, Ph.D.
Associate Professor of Pharmacology, Physiology and Biophysics

Second Reader

Ekaterina Kintsurashvili, PhD
Research Assistant Professor of Pharmacology, Physiology and
Biophysics.

DEDICATION

I would like to dedicate my work to my family. My parents, Lerma Lagason and Venerando Lagason, for raising me and allowing me to pursue my dreams. My sister, Inah Nicole Lagason, for being an inspiration that any younger sibling would be proud to have. I would also like to dedicate my work to my partner, Yifan Zhang, for the unwavering support she has provided.

ACKNOWLEDGMENTS

I would like to acknowledge the efforts of Dr. Hui Feng, MD, PhD, for introducing me to the field of cancer research and as a mentor. Her professionalism and expertise have made working alongside her an amazing experience and were defining characteristics in choosing to commit to the Feng Lab and this respective project.

I would like to express gratitude Dr. Ekaterina Kintsurashvili, PhD, as a reader for this thesis and faculty advisor during my time at Boston University.

I would also like to thank Abrar Ahmed, MS, AS, for his assistance throughout this project. His welcoming attitude and willingness to share knowledge in cell culture work, fluorescent staining, and overall wet lab skills has made this project possible.

To the members of the Feng Lab, I express my deepest gratitude for their companionship and support throughout the entirety of this thesis.

**ASSESSING ADAPTIVE CAPABILITIES
IN TRIPLE NEGATIVE BREAST CANCER CELLS
VAN MIGUEL LEOSALA LAGASON**

ABSTRACT

Objective: Our previous data suggests dihydrolipoamide S-succinyltransferase (DLST) as a key player in metabolic diversity within triple negative breast cancer (TNBC) cells. In metastatic TNBC, cellular stress can come from a multitude of sources, one of them being nutrient availability. The study aims to see how different TNBC cell lines, which are heterogenous in their expression of DLST, adapt to nutrient stress, specifically if there are changes in mitochondrial structure and cell viability.

Method: Two TNBC cell lines were chosen based on previous studies identifying their dependence or lack thereof on DLST. BT-549 and Hs578T are both epithelial cell lines that had originated from metastasized tumors. MCF10A is a cell line that was chosen as non-cancer control. Each cell line was subjected to a 48-hour starvation period post-seeding where they were measured for a cell viability and stained to analyzed mitochondrial morphology.

Results: After the glucose starvation period, DLST-dependent BT-549 cells were able to maintain a higher cell viability percentage at lowering glucose concentrations in comparison to DLST-independent Hs578T cells. Fluorescent analysis of stained cells showed significant mitochondrial fragmentation in DLST-independent cells while there were elongated mitochondria DLST-dependent cells.

Conclusion: The results support the idea that differences in DLST expression and dependency, are correlated to adaptive potential in TNBC cell lines. Specifically, DLST-dependent TNBC cell line BT-549 exhibited adaptive persistence in comparison to DLST-independent TNBC cell line Hs578T.

TABLE OF CONTENTS

DEDICATION	iv
ACKNOWLEDGMENTS	v
ABSTRACT.....	vi
TABLE OF CONTENTS.....	viii
LIST OF FIGURES	x
LIST OF ABBREVIATIONS.....	xii
INTRODUCTION	1
Breast cancer classifications and treatments.....	1
Cancer metabolism – target of interest	4
Mitochondrial fission and fusion	5
Introduction to DLST.....	8
Heterogeneity in DLST-dependency within TNBC cells.....	8
DLST influence on cellular pathways	9
OBJECTIVES	11
METHODS	12
Selection of Cell Lines.....	12
Determination of Starvation Period	12
Cell Culture.....	13
Cell Viability Assay.....	14
Fluorescence Staining and Imaging	15
RESULTS	17

TNBC cell lines with elevated DLST maintain cell viability	17
Mitochondrial structure is maintained in DLST-dependent TNBC cell line.....	22
DISCUSSION.....	37
CONCLUSION.....	42
BIBLIOGRAPHY.....	45
CURRICULUM VITAE.....	52

LIST OF FIGURES

Figure 1. MCF10A Cell Viability Bar	19
Figure 2. BT-549 Cell Viability Bar	20
Figure 3. Hs578T Cell Viability Bar graph	21
Figure 4. Comparative MitoTracker Red Fluorescence staining and imaging of MCF10A cells	23
Figure 5. MitoTracker Red Fluorescence staining and imaging of MCF10A cells at 3.151 g/L	24
Figure 6. MitoTracker Red Fluorescence staining and imaging of MCF10A cells at 0.315 g/L	25
Figure 7. MitoTracker Red Fluorescence staining and imaging of MCF10A cells at 0.158 g/L	26
Figure 8. Comparative MitoTracker Red Fluorescence staining and imaging of BT-549 cells	27
Figure 9. MitoTracker Red Fluorescence staining and imaging of BT-549 cells at 2.000 g/L	28
Figure 10. MitoTracker Red Fluorescence staining and imaging of BT-549 cells at 0.200 g/L	29
Figure 11. MitoTracker Red Fluorescence staining and imaging of BT-549 cells at 0.100 g/L	30
Figure 12. Comparative MitoTracker Red Fluorescence staining and imaging of Hs578T cells	31

Figure 13. MitoTracker Red Fluorescence staining and imaging of Hs578Tcells at 4.500 g/L.....	32
Figure 14. MitoTracker Red Fluorescence staining and imaging of Hs578Tcells at 0.450 g/L.....	33
Figure 15. MitoTracker Red Fluorescence staining and imaging of Hs578Tcells at 0.225 g/L.....	34
Figure 16. Comparative MitoTracker Red Fluorescence staining and imaging of dominant cell types in their base glucose concentrations	35
Figure 17. Comparative MitoTracker Red Fluorescence staining and imaging of all three cell lines in all nutrient conditions	36

LIST OF ABBREVIATIONS

DLST.....	Dihydrolipoamide S-Succinyltransferase
ER	Estrogen Receptor
HER2.....	Human Epidermal Growth Factor Receptor 2
OPA1.....	OPA1
OXPHOS.....	Oxidative Phosphorylation
PHB.....	Prohibitin
PR.....	Progesterone Receptor
TCA.....	Tricarboxylic Acid
TNBC.....	Triple Negative Breast Cancer

INTRODUCTION

Breast cancer classifications and treatments

Advancements in the early detection of breast cancer and its respective treatment have improved patient prognosis and lowered the mortality rate by 44% over the past thirty-three years (Giaquinto et al., 2024). The use of biomarkers and immunohistochemical analysis, has allowed for the discovery of distinct subtypes of breast cancer while targeted therapies rose from understanding their biological behaviors (Zaha 2014). Breast cancer is still one of the most common types of cancer worldwide, affecting millions of individuals every year and is the leading cancer diagnosis amongst women. Prevalence on a global scale continually begs the question and need for more efforts into understanding the disease and expanding the field of breast cancer research. Tumor behavior and available options for intervention often come down to the presence or absence of specific receptors found on the surface of breast cancer cells and the uncontrolled growth that comes from their activation.

The luminal subtypes (luminal A and luminal B) of breast cancers are highly influenced by steroid hormones due to a high amount of estrogen and/or progesterone receptors on the surface of the cells. Once steroid hormone-receptor complexes form and bind to response elements on DNA, an overactivation of genes occur that leads to cancerous growth (Orrantia-Borunda et al., 2022). Luminal B is known to have a more severe prognosis than luminal A and is often found through its aggressive metastatic behavior and increased concentration of proliferation biomarker Ki-67 (Inic et al., 2014). Together, estrogen receptor (ER) positive and progesterone receptor (PR) positive breast

cancers make up about 65% to 75% of breast cancers (Miah et al., 2019) (Zhang, et al., 2013).

Inspiration for targeted therapeutic intervention started as far back as the late 19th century with Beatson and the oophorectomy, believing ovaries act as a “controller” of the breast itself (Beatson 1896). Even before the discovery of estrogen itself in 1923, this work was foundational to modern day hormonal therapy. As we began to consider molecular therapies for luminal breast cancers, steroid hormone receptors became a prime target with selective receptor modulators and down regulators like tamoxifen and fulvestrant, respectively. Further innovation came in the form of preventing enzymatic conversion of androgens with aromatase inhibitors, such as letrozole. These treatments have benefitted patients and are seen to be more potent when combined with methods to address innate and acquired endocrine resistances (Goldner et al., 2021). Yet, mechanisms of tumor resistance can often occur through receptor mutations and upregulations of alternative pathways, requiring alternative treatment options (Alves et al., 2023).

Accounting for about 15% to 25% of breast cancers, human epidermal growth factor receptor 2 (HER2) positive cancers are characterized as faster-growing and more malignant than those of a luminal subtype (Asif et al., 2016). As a tyrosine kinase receptor, its activation leads to a cascade of signaling networks that include the PI3K/AKT/mTOR pathway, MAPK pathway, and JAK/STAT pathway, contributing to, cell proliferation, metastasis, and tumor resilience through immune evasion (Iqbal et al., 2014). First-line treatments focus on the HER2/neu protein on the surface of HER2

positive cancer cells directly. Monoclonal antibodies such as trastuzumab and pertuzumab have found success in preventing heterodimerization of the HER2 and thus signal transduction that would activate the previously mentioned pathways (Stanowicka-Grada et al., 2023). Early clinical phase trials have also seen success with antibody-drug conjugates and bispecific monoclonal antibodies which utilize the same monoclonal antibody technology to deliver cytotoxic drugs to cancer cells or recruit the immune system to detect cancer, respectively (Verma et al., 2013) (Bedard 2022). Similar to luminal cancers, HER2 positive tumors can develop primary and acquired resistance to targeted therapies (Sodergren et al., 2016). In few cases, extended use of monoclonal antibodies has caused cardiotoxicity, leading to cardiac damage and dysfunction (Sendur et al., 2013).

In about 10% to 15% of emerging breast cancers diagnoses are tumors that are not defined by the presence of ER, PR, or HER2 on their surface, but rather the lack thereof (Karim et al., 2023). TNBC poses an interesting challenge in comparison to the other subtypes. Without consistently identifiable receptors in each case of TNBC, our inability to apply receptor-based methodology establishes a need to research into the biological behavior and mechanisms that make TNBC unique and successful. It is understood that a mutation in the BRCA1 gene and its protein product can compromise DNA repair and lead to genomic instability that is commonly found in both hereditary and sporadic of cases of TNBC (Arun et al. 2024). First line treatments can often default to chemotherapy but often lead to a poor prognosis yet still retain a relatively high chance of relapse. Attempts to address the molecular pathway of the BRCA1 gene with Poly (ADP-ribose)

polymerase inhibitors are promising with their synthetic lethality but encounter tumor resistance in 40% to 70% of patients (Kim et al., 2022). Discovery of epidermal growth factor receptors on the surface of TNBC cells provides considerable potential for therapeutic inhibitors but is limited by their presence in only 60% of TNBC cases (Nielsen 2004).

In the same manner that distinguishes breast cancer types from each other, no two instances of breast cancer, even within classifications, are the same, leading to a highly heterogeneous disease (Takaoka et al., 2017). This heterogeneity, specifically within breast cancer subtypes, has influenced what current treatments are available. The inconsistencies amongst cancers within the “triple negative” subtype make it difficult to identify a consistent biomarker. This challenge begs the question for further investigation and understanding of the biological mechanisms that underlie TNBC.

Cancer metabolism – target of interest

Cellular respiration and the processes that allow cancer cells to meet their metabolic demands, especially in metastatic conditions, can provide insight to what contributes to their ability to maintain and grow. It has been shown that cancer cells can reprogram energy producing pathways in order to meet the demands of cell growth and movement (Patrick et al., 2012). TNBC in particular challenges clinicians with a lack in receptor-targeted therapeutic options, unlike the other types of breast cancers. Matched with its aggressive malignancy, there are relatively high rates of recurrence and poor overall prognosis for patients (Bianchini et al., 2016). Early studies have shown that 5

TNBC relies on aerobic glycolysis as a dominant source of energy production (Pelicano et al., 2014). More recent studies on metastatic TNBC have shown that there is a prominent switch from aerobic glycolysis to mitochondrial oxidative phosphorylation (OXPHOS) after analyzing patient-derived xenografts (Evans et al., 2021). OXPHOS dependency has continually grown to become a hallmark trait in spreading cancers. This has opened other opportunities to investigate dependency on other metabolic mitochondrial pathways in TNBC, such as the tricarboxylic acid (TCA) cycle, a major macromolecule contributor to OXPHOS.

Mitochondrial fission and fusion

Though they are classically known as the powerhouse of the cell, the mitochondria are highly dynamic in their structures and can take many different morphologies (Olichon, et al., 2002). With the mitochondria's involvement in a multitude of metabolic pathways, it has been linked to cell migration, cell cycle apoptosis, the production of ROS, and cell cycle apoptosis (Adebayo et al., 2022). In particular, the inner mitochondrial membrane folds in on itself to form cristae and is prominently known as the location that holds the enzyme complexes for OXPHOS (Zick et al., 2009). Like in many aspects of nature, structure can often influence function, especially how well or poorly that function takes place.

The efficiency of cellular respiration an overall growth and metastatic potential is influenced by mitochondrial structures (Blagov et al., 2024). Mitochondria contribute to this by undergoing changes in their structure by fusion and fission. In the case that a cell experiences stress, mitochondria can sustain damage, leading to a loss of efficiency or

overall function (Davis et al., 2014). Fusion relieves the effects of stress by providing complementation between damaged mitochondria, allowing one to compensate for the other and creating an elongated mitochondrion. In contrast, fission acts as a quality control mechanism, encouraging autophagy of damaged, fragmented mitochondria, and signaling the creation of new, healthy mitochondria. Fission also has a role of managing apoptosis when the cell undergoes considerable stress (Youle et al., 2012). During nutrient starvation, cells no longer have the available nutrients and macromolecules at their disposal. Thus, the amount of cAMP begins to increase, leading to the activation of protein kinase A. Once activated, a group of GTPases determine whether mitochondrial fusion or fission occurs. Optic atrophy 1 and dynamin-related protein 1 have been identified as genes and proteins of interest for fusion and fission, respectively (Baek et al., 2023). Therefore, analyzing mitochondrial structure, especially within cells that experience pressure from the make up of their microenvironment, provides insight to regulatory processes that can contribute to maintenance, growth, and proliferation.

A lack of balance between fission and fusion have been linked to a multitude of diseases such as cancer (Chan, 2009). Unimpeded fusion has been shown to create hyperfused amounts of mitochondria. These mitochondrial networks have been shown to have a higher OXPHOS capacity and persistence against autophagy in prolonged conditions of nutrient deficiency (Youle et al., 2012) (Gomes et al., 2011) (Sheng et al., 2014). Mice and cell culture studies have shown that fusion also reduces ROS production in TNBC, limiting any signaling to apoptotic pathways and encourages actin cytoskeleton reformation to promote cell migration. Those same models have shown that increased

mitochondrial fission shows the opposite and leads to more ROS production, reorganization of actin cytoskeleton structures that encourages apoptotic pathways, and prevention of TNBC migration (Humphries et al., 2023) (Shen et al, 2021).

Identifying and understanding what molecular interactions are involved with the OPA1 gene and resultant protein could be crucial to understanding metastatic potential. Prohibitins (PHB) are a group of highly conserved proteins that are expressed in multiple areas within the cell, including the nucleus, cytosol, and especially the mitochondria (Signorile et al., 2019). Though their presence can be found throughout the cell, the highest concentrations of PHBs are found within the mitochondria, along with most of their activity (Merkwith et al., 2009). PHBs carry a variety of functions, one of the most important being its part in OXPHOS. PHB1 and PHB2 form a PHB complex. This complex inhibits the *m*-AAA protease (Steglich et al., 1999) and OMA1 protease (McBride et al., 2010) from carrying out pro-apoptotic activity. The physical contact of the PHB complex with the proteases stabilizes itself and leads to the eventual stabilization of OPA1 (Ban et al., 2017). With OPA1 stabilized, cristae formation is incited allowing respiratory chain supercomplexes to properly form (Cogliati et al., 2013). Immunoblot analysis of PHB2 deficient cells has shown to produce unstable OPA1 isoforms. Fluorescent staining revealed an increase in fragmented mitochondria as a result. Introduction of functional OPA1 isoforms to PHB2 deficient cells were able to rescue them from defunct mitochondrial morphology and pro-apoptotic signaling (Merkwith et al., 2008). Though much has been documented about the behaviors of

OPA1 and PHB2, additional research is required to elucidate any activity of OPA1 and PHB2 with the components of metabolic pathways like the TCA cycle.

Introduction to DLST

The discovery of DLST can be traced to early studies on cellular respiration and specifically mitochondrial function. In the mid to late 20th century, the α -ketoglutarate dehydrogenase complex was discovered to consist of three subunits (Koike et al., 1973). DLST is one those three components that support the overall ability for the complex to irreversibly convert α -ketoglutarate to succinyl-CoA in the TCA cycle (Berg et al., 2002). As a transferase, it plays an important role in the transfer of succinyl units to a CoA substrate (Trefley et al., 2020). With improvements to our research techniques and tools, researchers were able to characterize its function and interactions with other biomolecules. Studies on those interactions have shown even shown differences in the expression of DLST and metabolic dependencies (Shen et al., 2021). As our understanding in DLST develops, so does its role in pathogenesis, tumor metabolism, and aggressive migration.

Heterogeneity in DLST-dependency within TNBC cells

In a recent study that aimed to compare the predictive capabilities of DLST and its 2 other subunits, dihydrolipoamide dehydrogenase and oxoglutarate dehydrogenase, DLST levels were able to reliably predict patient prognosis (Shen et al., 2021). Specifically, it was found that high levels of DLST anticipated cancer recurrence and poor overall survival in TNBC patients. The use of cell line models and protein analysis via western blotting, showed a lack of consistency in DLST protein expression amongst

TNBC cell lines. After standardizing base DLST levels using MCF10A, a nontumorigenic breast epithelial cell line, a collection of TNBC cell lines was found with differing levels of expression. To better understand TNBC pathogenesis, DLST knock-down testing was performed on both ER positive breast cell lines and TNBC cell lines via shRNA. All ER positive cell lines exhibited limited growth under DLST depletion. However, certain TNBC cell lines were found to be severely impacted by the DLST knock-down, while others were not. DLST-dependent TNBC cell line BT-549 had higher transcription and protein levels of DLST than that of Hs578T. DLST depletion in BT-549 cells showed a significantly lower growth rate. TNBC cell lines of those lower with DLST expression, like Hs578T, experienced little change in their growth rates, making their metabolic potential independent of DLST expression. The same study found that zebrafish xenografts with transplanted with BT-549 cells were seen to have less tumor burden and invasion under DLST depletion (Shen et al., 2021). Further immunofluorescent staining of those cell lines showed that the knock-down had also induced mitochondrial reactive oxygen species (ROS). At homeostatic levels, ROS act as secondary messengers in many biomolecular pathways, yet excessive and imbalanced amounts of ROS can degrade DNA, proteins, and lipids, leading to cell death or even altered cell function (Shields et al., 2021). Further understanding of DLST and the effects on cell structure and function have the potential to uncover novel molecular interactions.

DLST influence on cellular pathways

Amongst energy-producing pathways, it is recognized that TCA cycle predominantly takes place within the mitochondrial matrix (Alabduladhem et al., 2022).

Our previous studies have compared the functionality between DLST-dependent and independent cell lines by replacing glucose with galactose, to encourage to TCA cycle usage over glycolysis within the cytoplasm (Robinson, 1992). Our evaluation showed that DLST-dependent cell lines were able to maintain homeostatic levels of ATP without being significantly affected. Cell lines with a lower expression or dependency on DLST were found with lower levels of ATP when grown in galactose supplemented media. (Shen et al., 2021). This demonstrates that TNBC cell lines carry out and utilize on the TCA cycle in different capacities, showing that cell line dependency on DLST and sensitivity to microenvironment change is heterogeneous.

DLST-depletion via knock-down also showed changes in other pathways, aside from the TCA cycle. Metabolomics profiling showed other redox regulating pathways being altered in DLST-dependent cell line BT-549. This included the metabolism of cysteine and methionine. Cysteine levels decrease while there was an increase in other metabolites such as, methionine, cystine, and S-adenosyl-L-methionine. The pentose phosphate pathway was also seen to have been disturbed. Concentrations of 5-phosphoribosyl-1-pyrophosphate decreased while, D-erythrose-4-phosphate, glucose-6-phosphate, and 6-phospho-D-gluconate levels increased (Shen et al., 2021). This influence on cellular metabolites suggests that DLST may play an important role in maintaining energy producing pathways, redox balance, and cellular viability, especially when under stress.

OBJECTIVES

In malignant tumors, the change in microenvironments often places intense stress on cells. This stress can come in the form of leaving the initial primary site, enduring the pressure of traveling through blood vessels, and reaching a secondary destination where it will not only have to adjust to new surroundings, but as well as avoid components of the immune system (Massagué et al., 2016). What accompanies the change in environments is also challenges of energy demand, macromolecule availability, and potential redox imbalance (Anderson et al., 2014). Yet, TNBC can persist. Thus far, the difference in adaptive capabilities within TNBC cell lines, specifically under nutrient stress remains relatively undetermined.

This study means to build upon our previous research and study the adaptive capabilities of TNBC cell lines. Ultimately, we seek to better understand the molecular interactions of DLST and how heterogeneity of DLST-dependence between TNBC cell lines can influence cell growth, viability, and mitochondrial morphology. For this study, we hypothesize that DLST-dependent TNBC cell lines, such as BT-549, will adapt to nutrient stress with a higher percentage of viable cells and less fragmented mitochondria over the starvation period. We also predict that DLST-independent TNBC cell line Hs578T will have lower percentage of viable cells over the starvation period and more fragmented mitochondria. This would be consistent with the previous studies and the current evidence of DLST (Shen et al., 2021). profound text of my dissertation goes here.

METHODS

Selection of Cell Lines

Two TNBC cell lines were chosen based on previous studies identifying their dependence or lack thereof on DLST. BT-549 and Hs578T are both epithelial cell lines that had originated from metastasized tumors. These two cell lines pose as ideal candidates for comparison because of their differing base levels of DLST that was discovered by western blot analysis and determination of their dependency on it via knock-down testing (Shen et al 2021). MCF10A was chosen as the third cell line, acting as a nontumorigenic control. MCF10A was also the original cell line that was used for relative comparison of DLST protein expression in the western blot analysis. BT-549 had shown to have a relative DLST protein expression level that was closer to MCF10A and higher than Hs578T. Hs578T contains relatively lower levels of DLST in comparison to MCF10A and BT-549. DLST depletion via knock-down showed significantly lower growth rates, increased apoptosis and necrosis signaling in BT-549 cells, suggesting their dependency on DLST. Those same metrics showed minimal effect in Hs578T cells, showing little evidence of DLST-dependency (Shen et al., 2021).

Determination of Starvation Period

Prior to any cell seeding and cultivation, a set starvation time and nutrient conditions must be established. The intention was to create an experimental condition that mimicked a change in the microenvironments after TNBC had migrated from its primary tumor, subjecting the cells to acute starvation and cellular stress. The period of this stress should be long enough to encourage metabolic remodeling from aerobic

glycolysis to OXPHOS without large alterations in protein expression. Prolonged periods of starvation would lead to mass apoptotic signaling and end in a lack of tangible data for comparison and analysis. BT-549, Hs578T, and MCF10A are all adherent cell lines and require time to properly attach to plate surfaces, each with duplication times of 21-hours to 26-hours. Serum starvation studies noted experiences with 24-hour, 48-hour, and 72-hour starvation periods (Rashid et al., 2018) (Zeidler et al., 2017). In our experiments, 48-hours was able to satisfy all the previously stated conditions. It ensured proper adherence of the cells to the seeded surfaces. There would also be sufficient time in growth media that corresponds to their doubling time and allow for proliferation without the risk of contact inhibition due to confluency.

Cell Culture

Three cell lines were received from the American Type Culture Collection (www.atcc.org), seeded onto 75 cm² U-shape cell culture flasks, and cultured at 37 °C supplemented with 5% CO₂. MCF10A cells were cultured in DMEM/F12 medium with a glucose concentration of 3.151 g/L (SH30023.FS, Hyclone) and supplemented with 5% horse serum (26-050-088, Fisher Scientific), 20 ng ml⁻¹ epidermal growth factor (E4127, Sigma), 100 ng ml⁻¹ cholera toxin (C8052, Sigma), 10 ng ml⁻¹ insulin (I9278, Sigma), and 500 ng ml⁻¹ hydrocortisone (H4001, Sigma) (Imbalzano et al., 2009). Hs578T cells were cultured in DMEM medium with a glucose concentration of 4.500 g/L (MT10013CV, Corning) and supplemented with 10% fetal bovine serum (FBS, F0926, Sigma), as recommended by the ATCC. BT-549 cells were cultured in RPMI 1640 medium with a glucose concentration of 2.000 g/L (MT10040CV, Corning) and

supplemented 10% FBS, as recommended by the ATCC. Following typical cell passage protocols, all cell lines were maintained, and trypsinized to prevent confluency, and contact inhibition. A hemocytometer was used to determine the concentration of cells per milliliter prior to seeding for experimentation.

Cell Viability Assay

In a 96-well clear-bottom, black plate, a total of 10 columns contained that adjusted complete growth media that corresponded to each cell line. Glucose-containing media was diluted with non-glucose containing media to make a gradient of glucose concentrations in eight columns, along with two columns that contained glucose free media. The highest glucose concentrations started with a 4.500 g/L and were serially diluted by half each time to as low of a concentration of 0.035 g/L.

One of the glucose-free columns was assigned to contain only growth media without cells, totaling a volume of 100 microliters. This column will serve as a negative control whose fluorescence will be used to calculate cell viability. The remaining glucose-free column and the eight columns of media with differing glucose concentrations were seeded with 5,000 cells (50 cells per microliter), totaling a volume of 100 microliters. 200 microliters of sterile water were added to each well on the edge of the plate. Wells on the edge of the plate were void of any media and cells to prevent the effects of evaporation and inconsistencies in measuring fluorescence (Mansoury et al., 2021).

After the initial seeding, the plate was placed in a 5% CO₂ humidified incubator at 37°C for 48-hours. After the 48-hour starvation period, cells were stained following the

CellTiter-Blue® Cell Viability Assay (G8080, Promega) protocol. 20 microliters of CellTiter-Blue were added to each well and incubated for 4-hours. The use of an indicator dye allowed us to measure the metabolic capacity of the cells, specifically on how well they can retain their metabolic activity post-starvation period. The reagent contains high amounts of resazurin, which by itself is poorly fluorescent dye. However, it can be reduced to resorufin in metabolically active cells. Resorufin emits light at 590 nanometers in which fluorescence can be measured and used to determine cell viability (Gloeckner et al., 2001). Fluorescence values were recorded by CLARIOstar Plus microplate reader and analyzed to convey cell viability percentages.

Fluorescence Staining and Imaging

All cell lines were seeded onto sterile coverslips and cultured in three different glucose concentrations, a starting glucose concentration determined by the concentration of the base medium that was used, a 1:10 dilution, and 1:20 dilution. DMEM/F12 (SH30023.FS, Hyclone) medium has a D-glucose concentration of 3.151 grams per liter (g/L). MCF10A cells were seeded onto sterile coverslips in the following glucose concentrations, 3.151 g/L, 0.315 g/L, and 0.158 g/L. DMEM medium has a D-glucose concentration of 4.500 g/L. Hs578T cells were seeded onto sterile coverslips in the following glucose concentrations, 4.500 g/L, 0.450 g/L, and 0.225 g/L. RPMI 1640 medium has a D-glucose concentration of 2.000 g/L. BT-549 cells were seeded onto sterile coverslips in the following glucose concentrations, 2.000 g/L, 0.200 g/L, and 0.100 g/L.

After the 48-hour starvation period, the cells were treated with MitoTracker™ Red CMXRos (M7512, Thermofisher), according to the instructions provided by the manufacturer. The dye enters the mitochondria by diffusion and covalently binds to proteins in the mitochondria, activating the fluorescence in the probe. After 30 minutes of incubation, the cells were thoroughly washed with Dulbecco's Phosphate Buffered Saline (SH30028LS, Corning), and were fixed with 4% paraformaldehyde (158127, Sigma) at room temperature for 10 minutes. Once fixation was complete, the paraformaldehyde was removed, and the coverslip was washed again with Dulbecco's Phosphate Buffered Saline. Cells were then mounted onto glass slides (12-550-15, Fisher Scientific) using VECTASHIELD® Antifade Mounting Medium (H-1000-10, Vector Laboratories). Images were taken using RVL-100-G microscope (ECHO) under 60X magnification with immersion oil (MXA22203, Nikon).

RESULTS

TNBC cell lines with elevated DLST maintain cell viability

Previous studies have shown that human TNBC cell lines express unequal dependence on DLST and how high levels of DLST can predict poor overall patient outcomes (Shen et al., 2021). Our starvation studies support the idea that DLST influences metabolic activity and holds a key role in maintaining metabolic potential, especially when under nutrient stress (Figure 1, Figure 2 Figure 3).

The MCF10A cells, though non-tumorigenic, have protein and transcript levels of DLST that have been used as a relative comparison to TNBC cell lines (Shen et al., 2021). After the starvation period, MCF10A cells treated with 4.5000 g/L showed a significant, higher cell viability compared to cells treated with lower glucose concentrations or a glucose free condition, with viability decreasing by approximately 14% ($p = 0.0330$), 17% ($p = 0.0203$), 33% ($p = 0.0022$), and 37% ($p = 0.0010$), respectively in the 0.1406 g/L, 0.0703 g/L, 0.0351 g/L glucose and glucose-free conditions.

The BT-549 cells express levels of DLST that are higher than that of Hs578T and closer to that of MCF10A and are characterized as DLST-dependent (Shen et al., 2021). After the starvation period, BT-549 cells treated with 4.5000 g/L showed a significant, higher cell viability compared to cells treated with lower glucose concentrations or a glucose free condition, with viability decreasing by approximately 16% ($p = 0.0325$), 44% ($p = 0.0001$), 47% ($p < 0.0001$), respectively in the 0.2812 g/L, 0.0351 g/L, and the glucose free condition (Figure 2).

The Hs578T cells express comparatively lower levels of DLST than that of MCF10A and BT-549 and is designated as DLST-independent (Shen et al., 2021). After the starvation period, Hs578T cells treated with 4.5000 g/L glucose showed a significant higher cell viability compared to cells treated with lower glucose concentrations or a glucose-free condition, with viability decreasing by approximately 51%, ($p = 0.0006$), 71% ($p = 0.0002$), (79% $p < 0.0001$), (81%, $p < 0.0001$), 87% ($p < 0.0001$) respectively in the 0.2812 g/L, 0.1406 g/L, 0.0703 g/L, 0.0351 g/L, and the glucose-free condition (Figure 3).

MCF10A

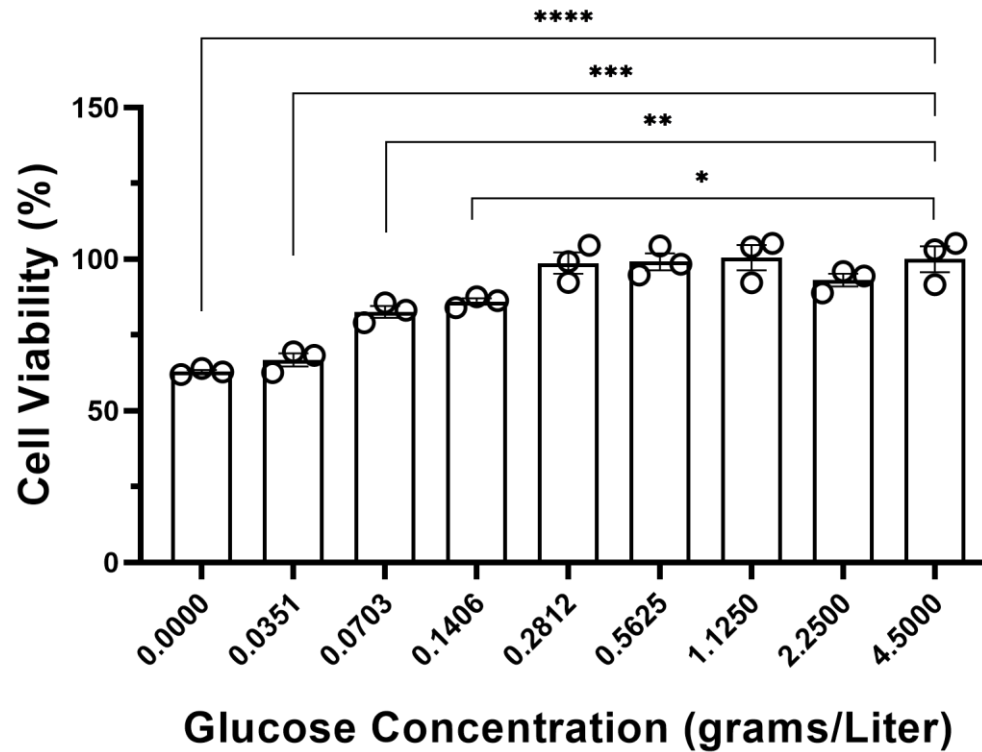


Figure 1. MCF10A Cell Viability Bar graph depicting calculated cell viability percentage across serially diluted glucose concentrations and a glucose-free condition. Bars represent the mean \pm SEM, with individual data points overlaid. Statistical significance ($p < 0.05$) was determined using unpaired t-test against the control group (4.500 g/L). Significance was discovered in the 0.1406 g/L ($p = 0.0330$), 0.0703 g/L ($p = 0.0203$), 0.0351 g/L ($p = 0.0022$), and the glucose-free ($p = 0.0010$) conditions.

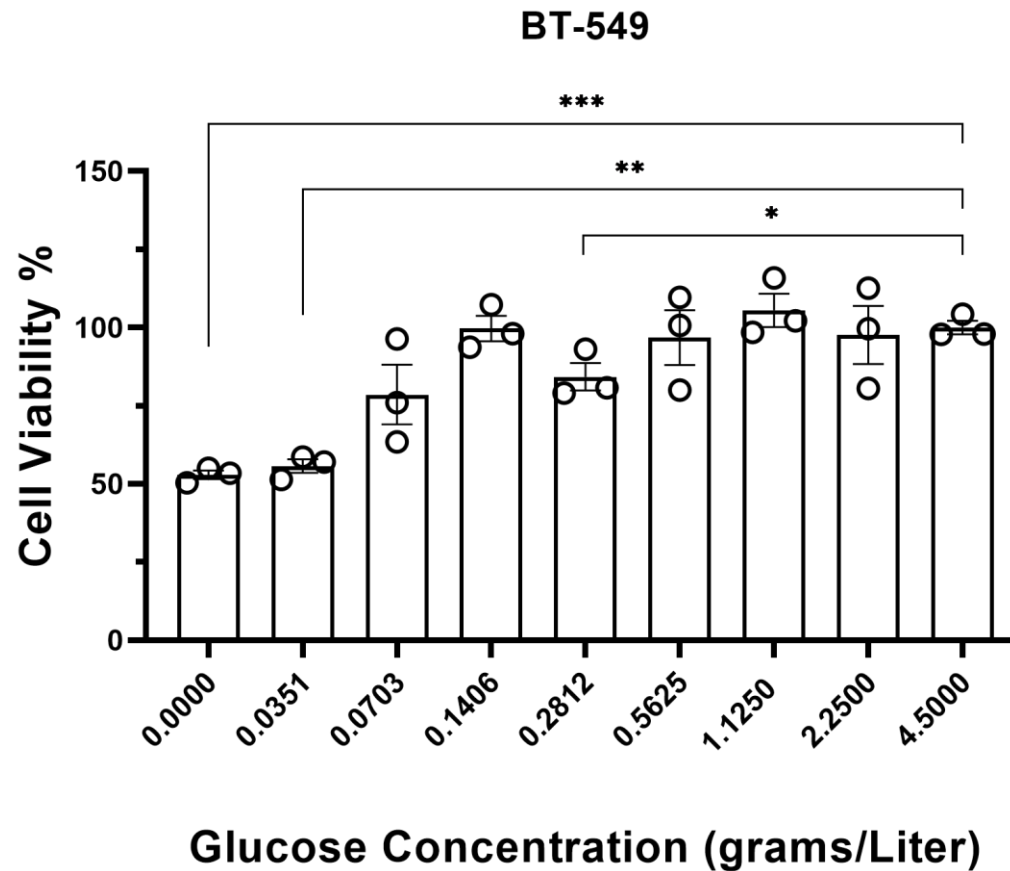


Figure 2. BT-549 Cell Viability Bar graph depicting calculated cell viability percentage across serially diluted glucose concentrations and a glucose-free condition. Bars represent the mean \pm SEM, with individual data points overlaid. Statistical significance ($p < 0.05$) was determined using unpaired t-test against the control group (4.500 g/L). Significance was discovered in 0.2812 g/L ($p = 0.0325$), 0.0351 g/L ($p = 0.0001$), and the glucose-free ($p = <0.0001$) conditions.

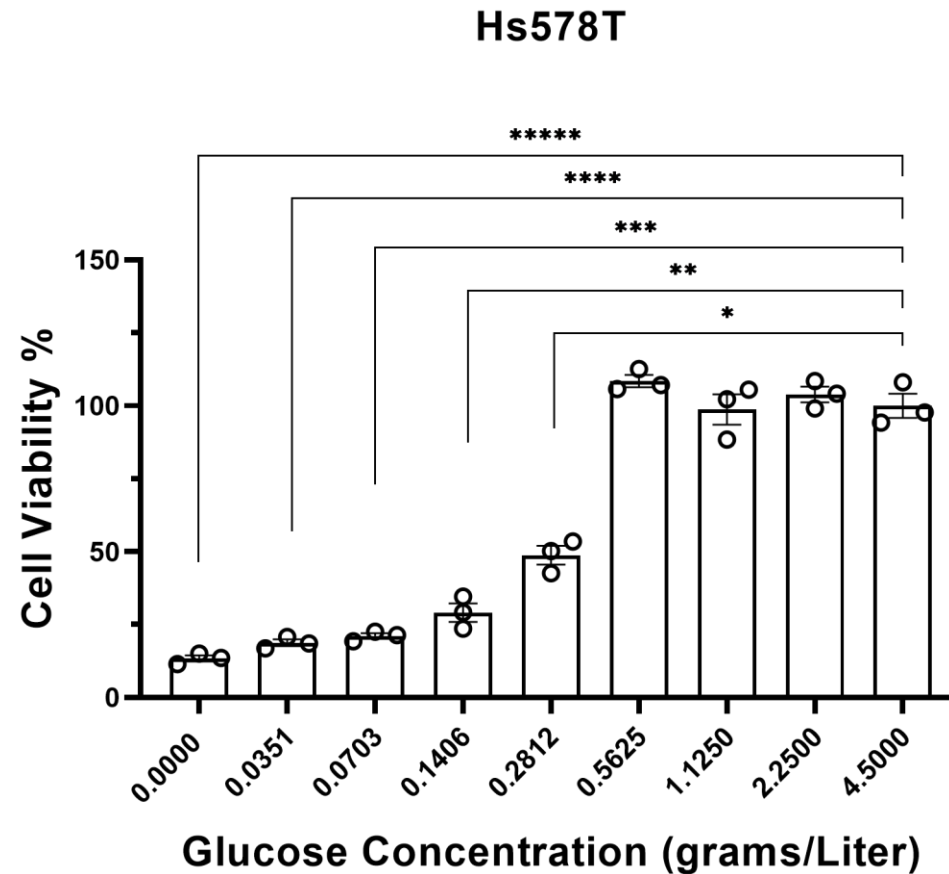


Figure 3. Hs578T Cell Viability Bar graph depicting calculated cell viability percentage across serially diluted glucose concentrations and a glucose-free condition. Bars represent the mean \pm SEM, with individual data points overlaid. Statistical significance ($p < 0.05$) was determined using unpaired t-test against the control group (4.500 g/L). Significance was discovered in the 0.2812 g/L ($p = 0.0002$), 0.1406 g/L ($p = 0.0001$), 0.0703 g/L ($p = < 0.0001$), 0.0351 g/L ($p = < 0.0001$), and the glucose-free ($p = < 0.0001$) conditions.

Mitochondrial structure is maintained in DLST-dependent TNBC cell line

Our previous studies have shown that knock-down studies of DLST have shown increased mitochondria dysfunction DLST-dependent TNBC cell lines. We sought to understand how stress would affect mitochondria, as changes in function often goes in tandem with structural integrity and morphology. Under nutrient stress, we observed differences in how well different TNBC cell lines could adapt based on their expression of DLST. Using ECHO, we able to take images of mitochondrial structure under differing levels of nutrient stress. Our images showed that MCF10A maintained highest frequency of elongated mitochondria and elaborate mitochondrial networks amongst all cell lines under acute nutrient stress (Figure 4, Figure 5, Figure 6, Figure7, Figure 17). In contrast, Hs578T had predominantly fragmented mitochondria in all three glucose concentrations, increasing in their circularity and decreasing in their overall length (Figure 8, Figure 9, Figure 10, Figure 11, Figure 17). BT-549 cells contained elongated mitochondria at a high frequency in all three glucose concentrations (Figure 12, Figure 13, Figure 14, Figure 15, Figure 17). Even at their assigned highest concentration 3.151 g/L for MCF10A, 4.500 g/L for Hs578T, and 2.000 g/L for BT-549, Hs578T had a lower frequency of cells with elongated mitochondria and the highest percentage of fragmented mitochondria (Figure 16).

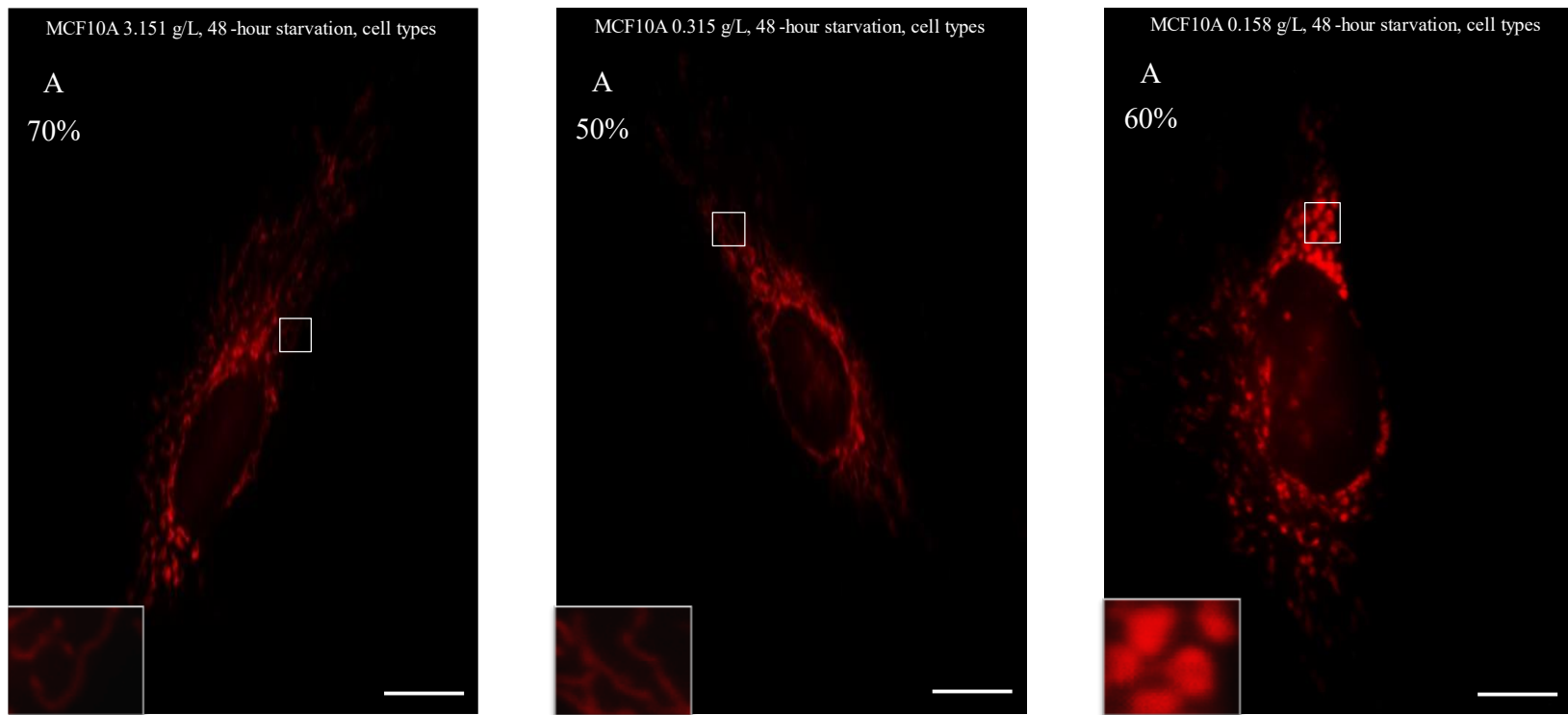


Figure 4. Comparative MitoTracker Red Fluorescence staining and imaging of MCF10A cells Each image represents the most common cell type observed in each glucose concentration, A (3.151 g/L), B (0.315 g/L), and C (0.158 g/L), along with an approximation of its overall percentage on their respective slides. Each image was taken at 60X magnification with immersion oil.

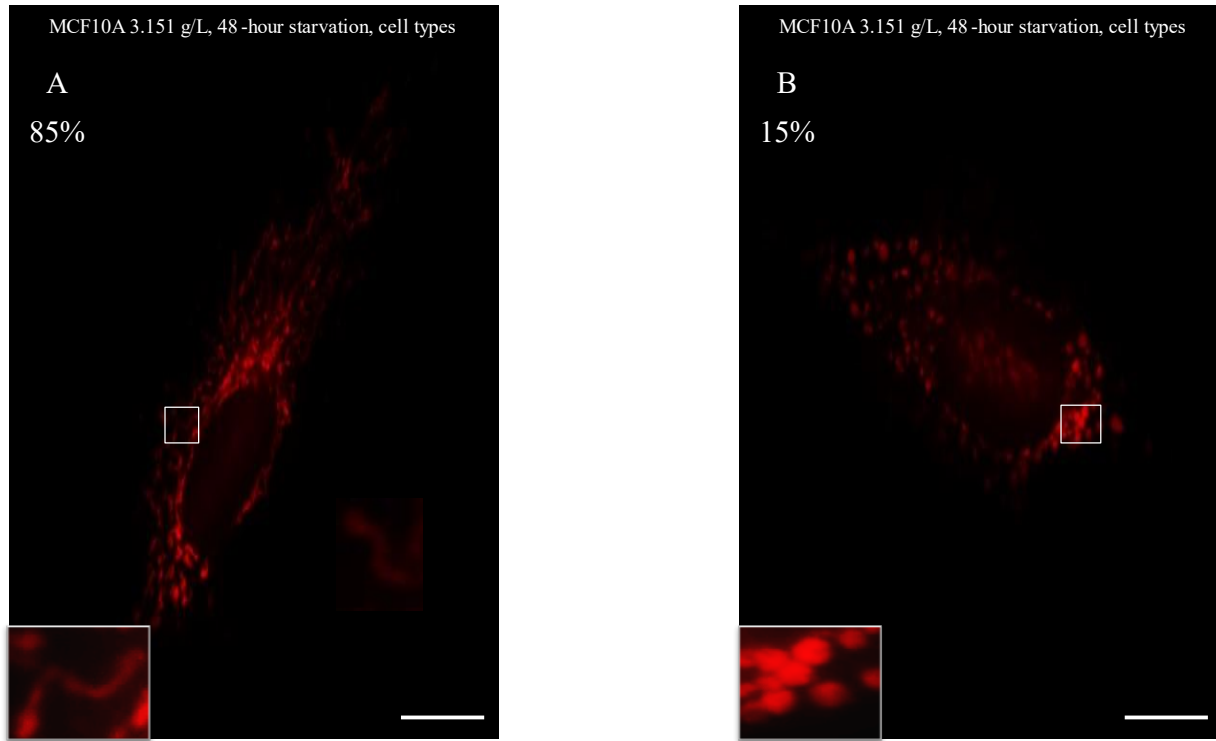


Figure 5. MitoTracker Red Fluorescence staining and imaging of MCF10A cells at 3.151 g/L Representative cell types were chosen to describe the mitochondrial makeup of the entire coverslip seeded with a glucose concentration of 3.151 g/L. Each image was taken at 60X magnification with immersion oil and highlights elongated or shattered mitochondria with their respective frequencies in percentages (A and B).

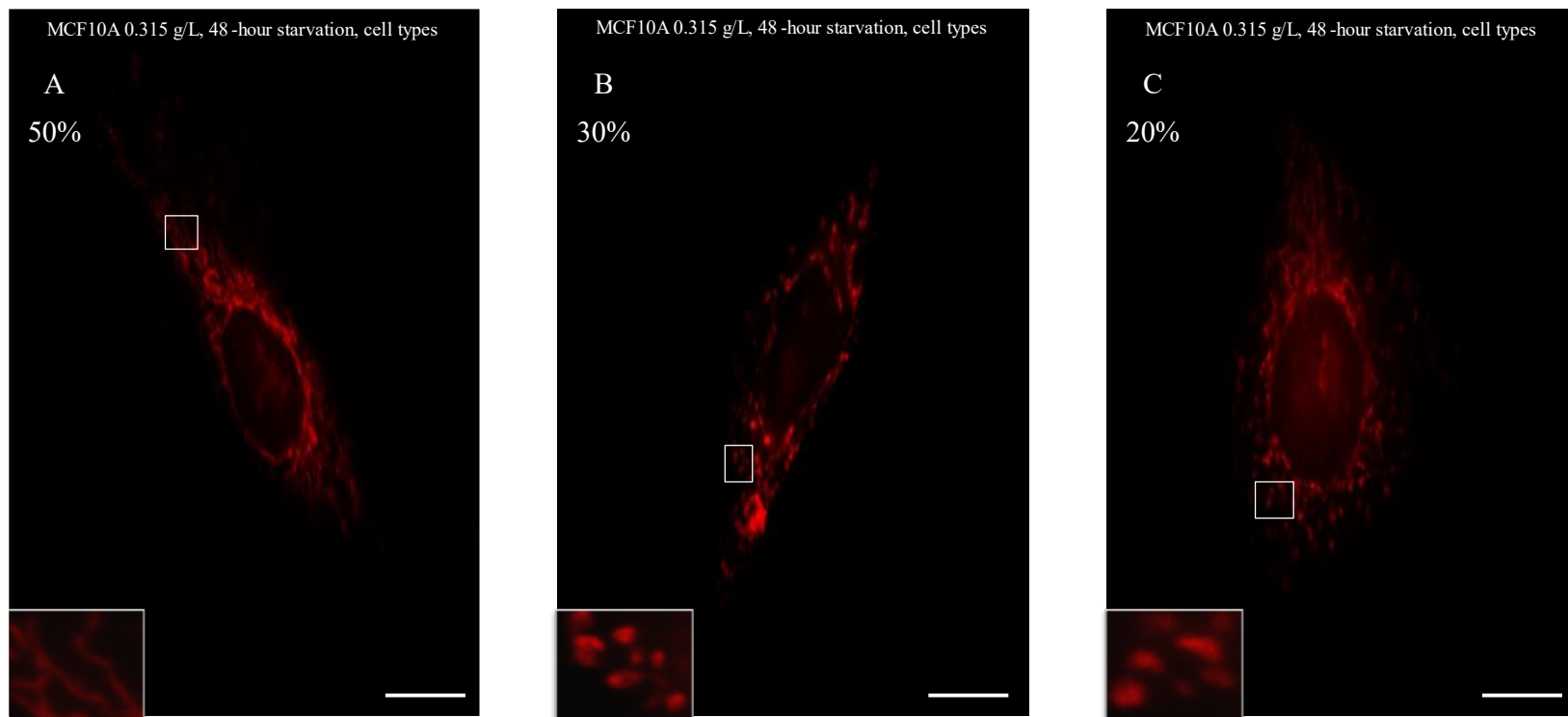


Figure 6. MitoTracker Red Fluorescence staining and imaging of MCF10A cells at 0.315 g/L Representative cell types were chosen to describe the mitochondrial makeup of the entire coverslip seeded with a glucose concentration of 0.315 g/L. Each image was taken at 60X magnification with immersion oil and highlights elongated or shattered mitochondria with their respective frequencies in percentages (A, B, and C).

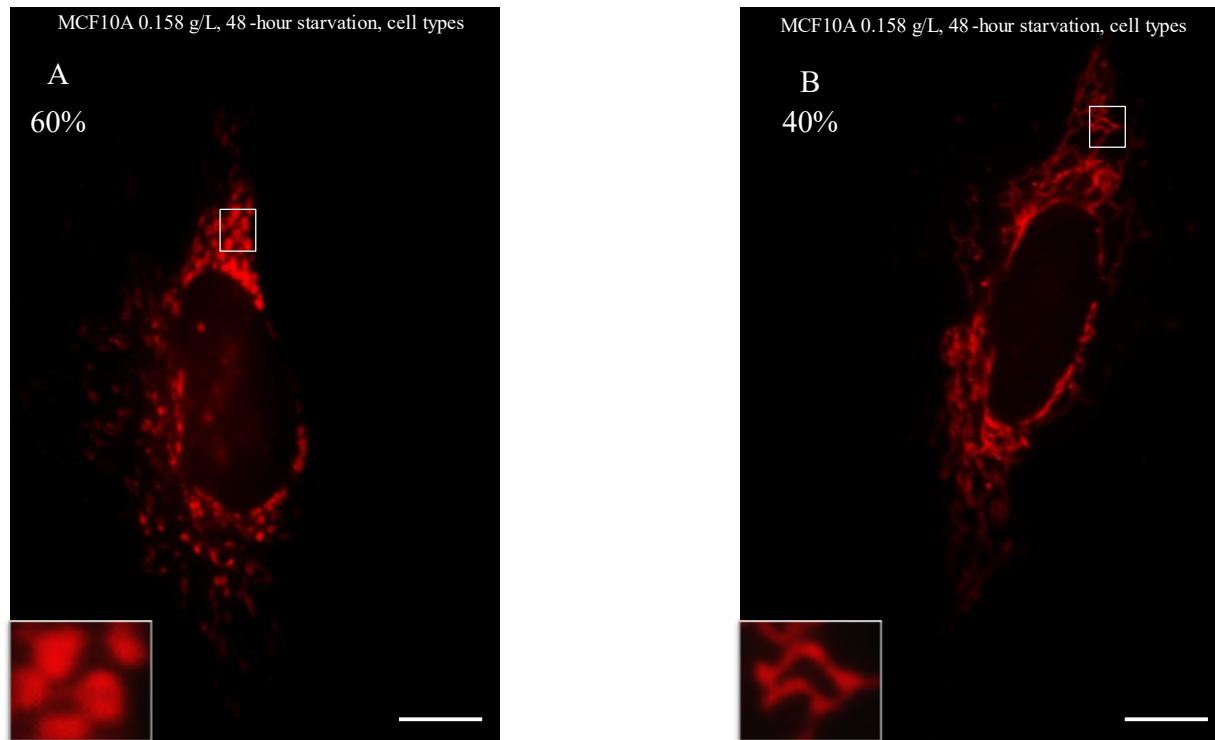


Figure 7. MitoTracker Red Fluorescence staining and imaging of MCF10A cells at 0.158 g/L Representative cell types were chosen to describe the mitochondrial makeup of the entire coverslip seeded with a glucose concentration of 0.158 g/L. Each image was taken at 60X magnification with immersion oil and highlights elongated or shattered mitochondria with their respective frequencies in percentages (A and B).

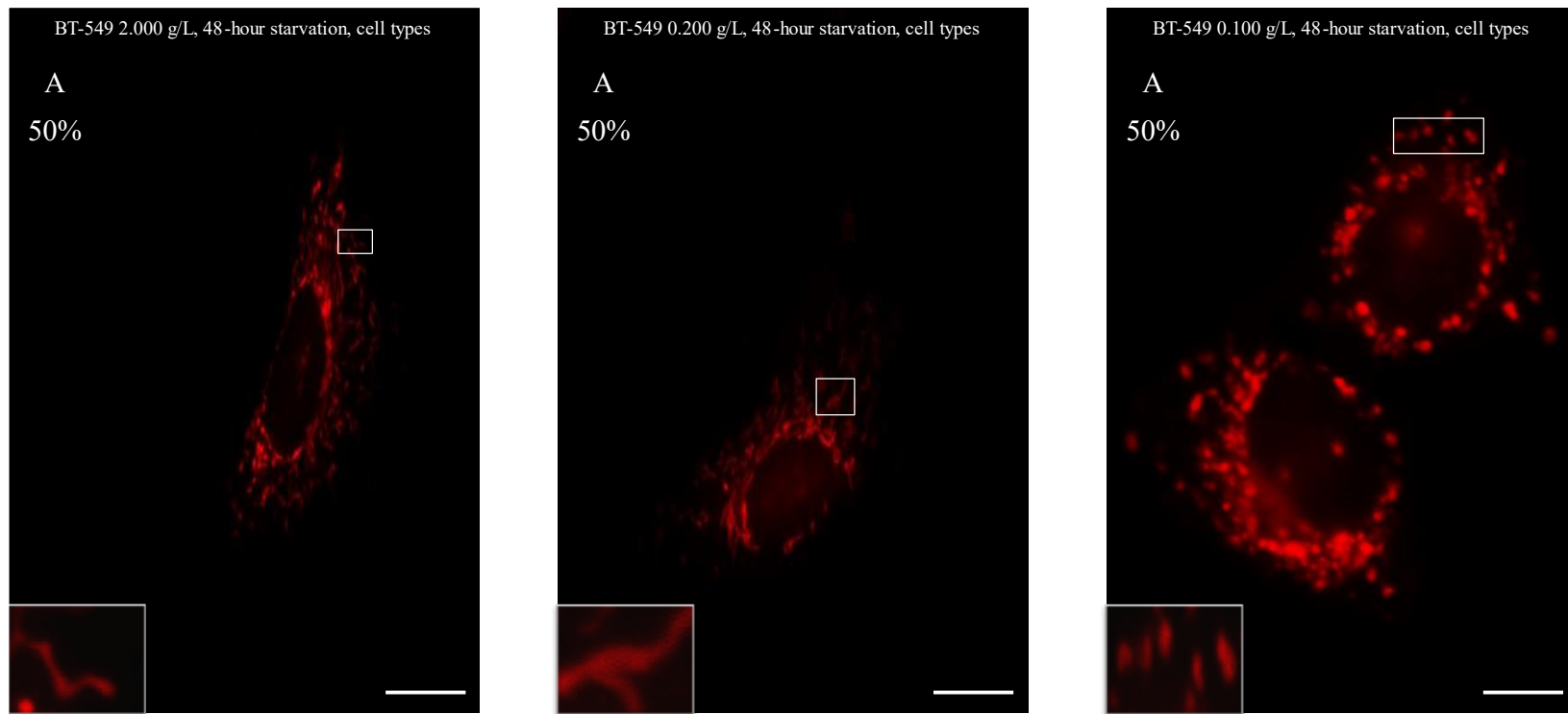


Figure 8. Comparative MitoTracker Red Fluorescence staining and imaging of BT-549 cells Each image represents the most common cell type observed in each glucose concentration, A (2.000 g/L), B (0.200 g/L), and C (0.100 g/L), along with an approximation of its overall percentage on their respective slides. Each image was taken at 60X magnification with oil.

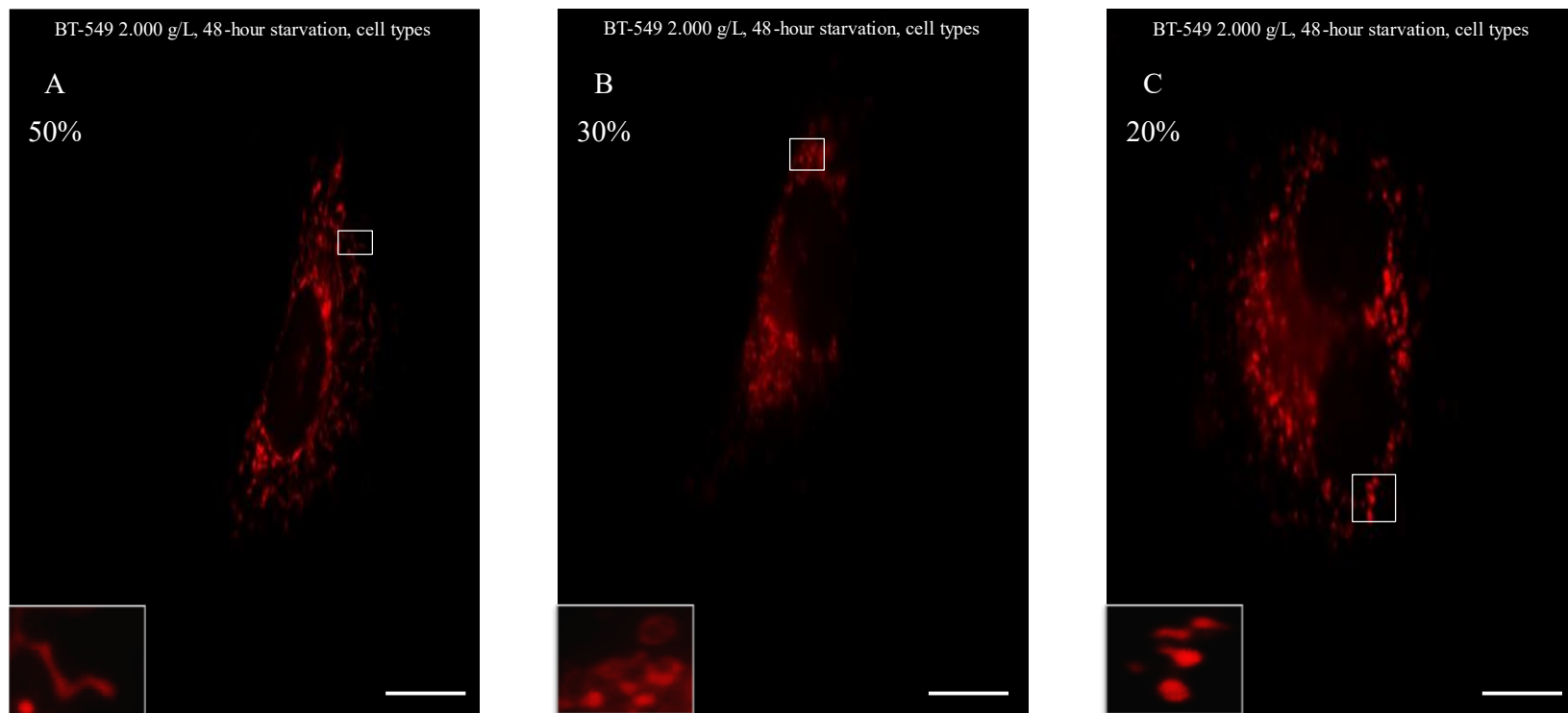


Figure 9. MitoTracker Red Fluorescence staining and imaging of BT-549 cells at 2.000 g/L Representative cell types were chosen to describe the mitochondrial makeup of the entire coverslip seeded with a glucose concentration of 2.000 g/L. Each image was taken at 60X magnification with immersion oil and highlights elongated or shattered mitochondria with their respective frequencies in percentages (A, B and C).

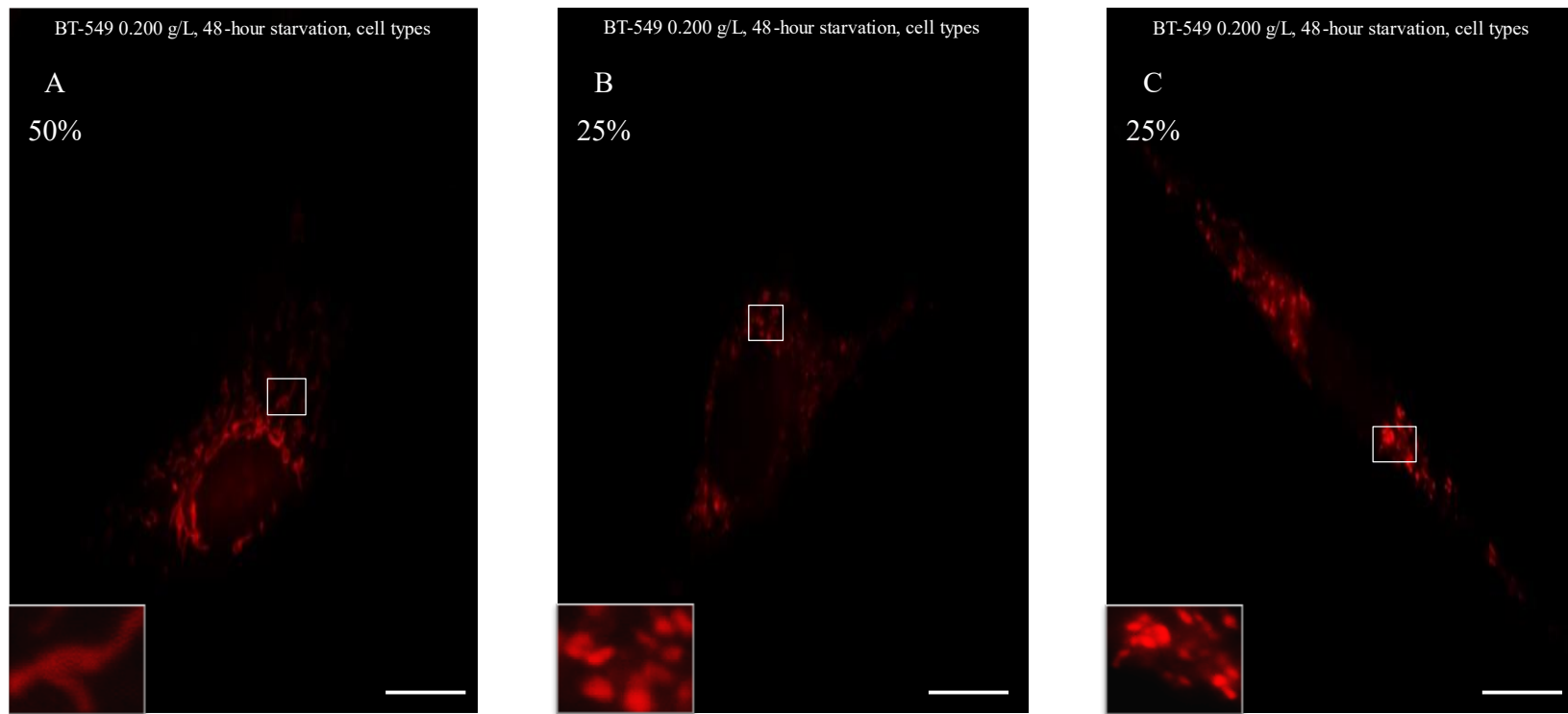


Figure 10. MitoTracker Red Fluorescence staining and imaging of BT-549 cells at 0.200 g/L Representative cell types were chosen to describe the mitochondrial makeup of the entire coverslip seeded with a glucose concentration of 0.200 g/L. Each image was taken at 60X magnification with immersion oil and highlights elongated or shattered mitochondria with their respective frequencies in percentages (A, B, and C)

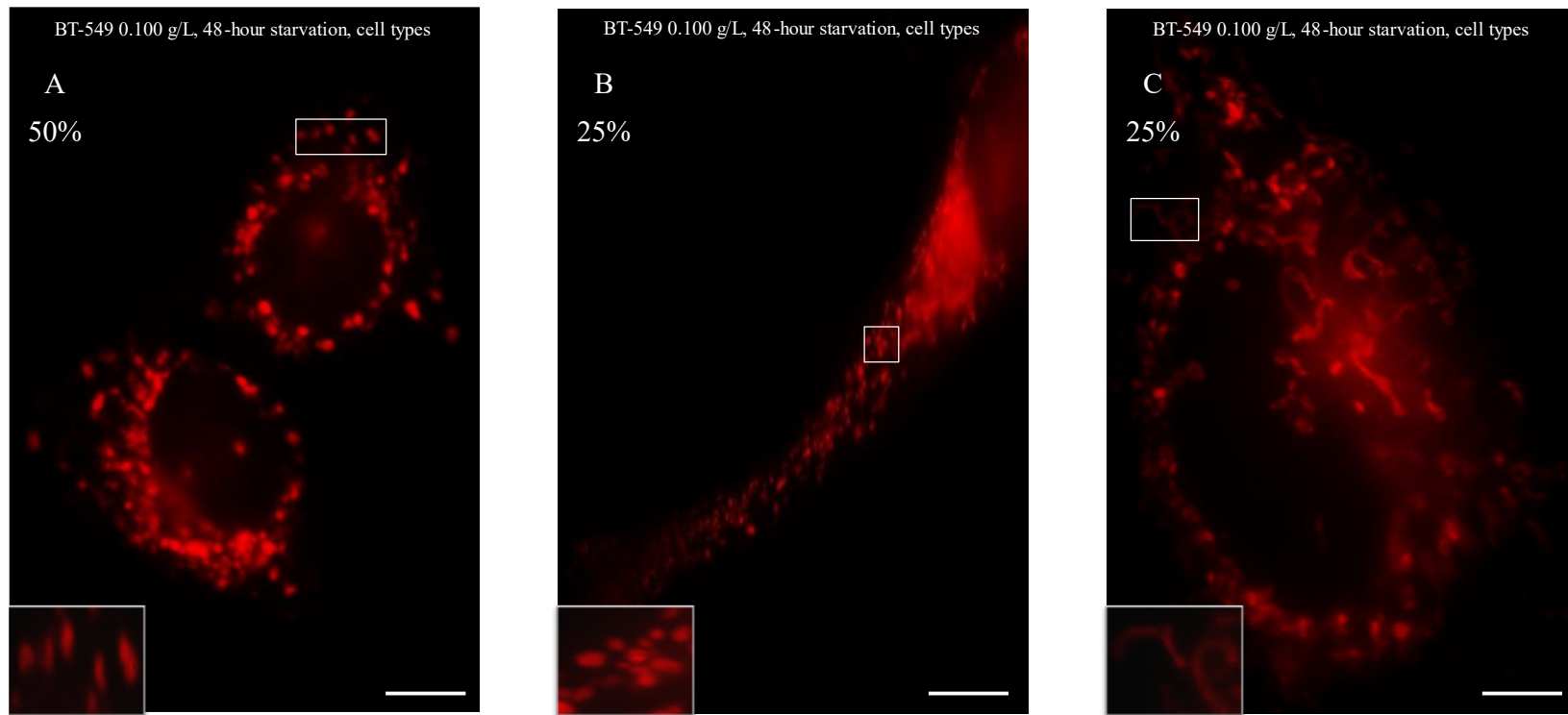


Figure 11. MitoTracker Red Fluorescence staining and imaging of BT-549 cells at 0.100 g/L Representative cell types were chosen to describe the mitochondrial makeup of the entire coverslip seeded with a glucose concentration of 0.100 g/L. Each image was taken at 60X magnification with immersion oil and highlights elongated or shattered mitochondria with their respective frequencies in percentages (A, B, and C).

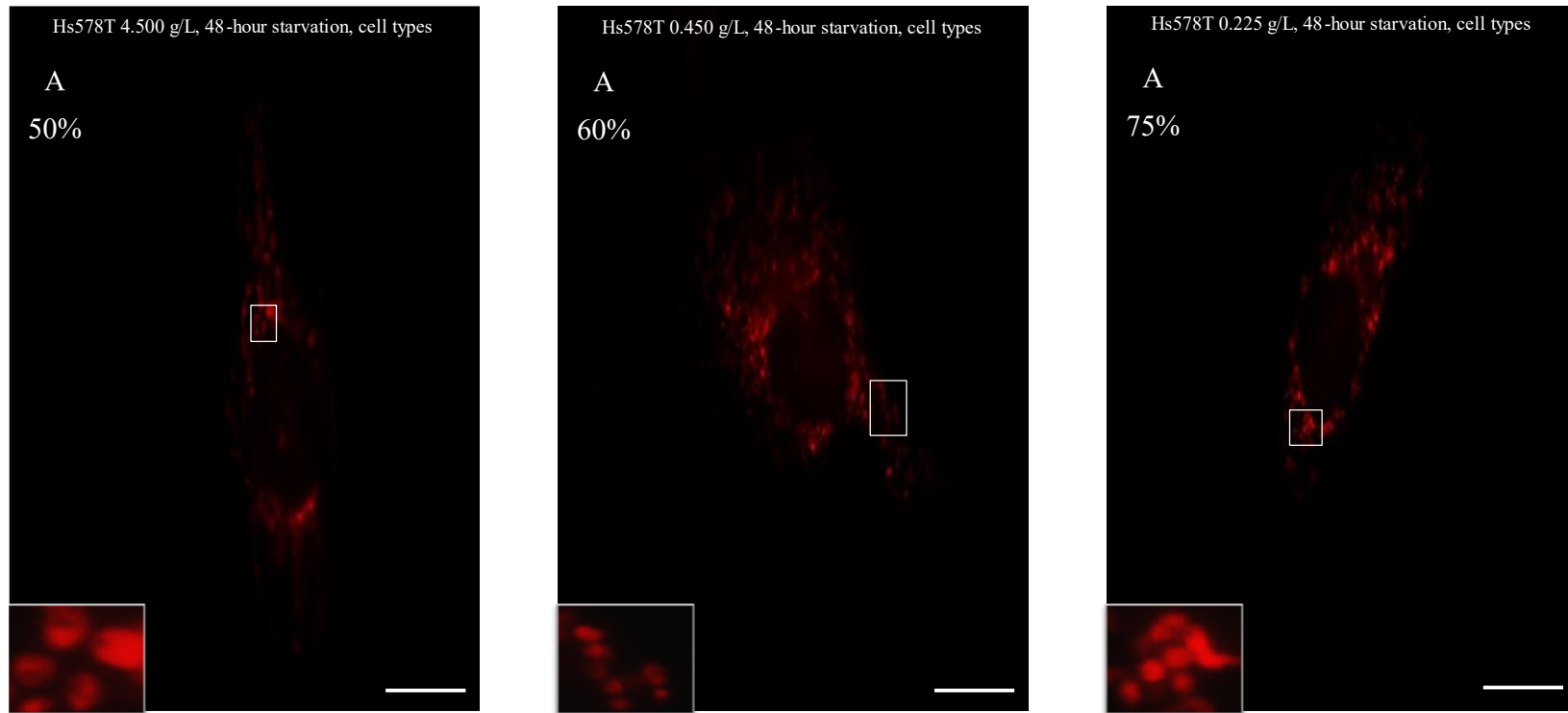


Figure 12. Comparative MitoTracker Red Fluorescence staining and imaging of Hs578T cells Each image represents the most common cell type observed in each glucose concentration, A (4.500 g/L), B (0.450 g/L), and C (0.225 g/L), along with an approximation of its overall percentage on their respective slides. Each image was taken at 60X magnification with oil.

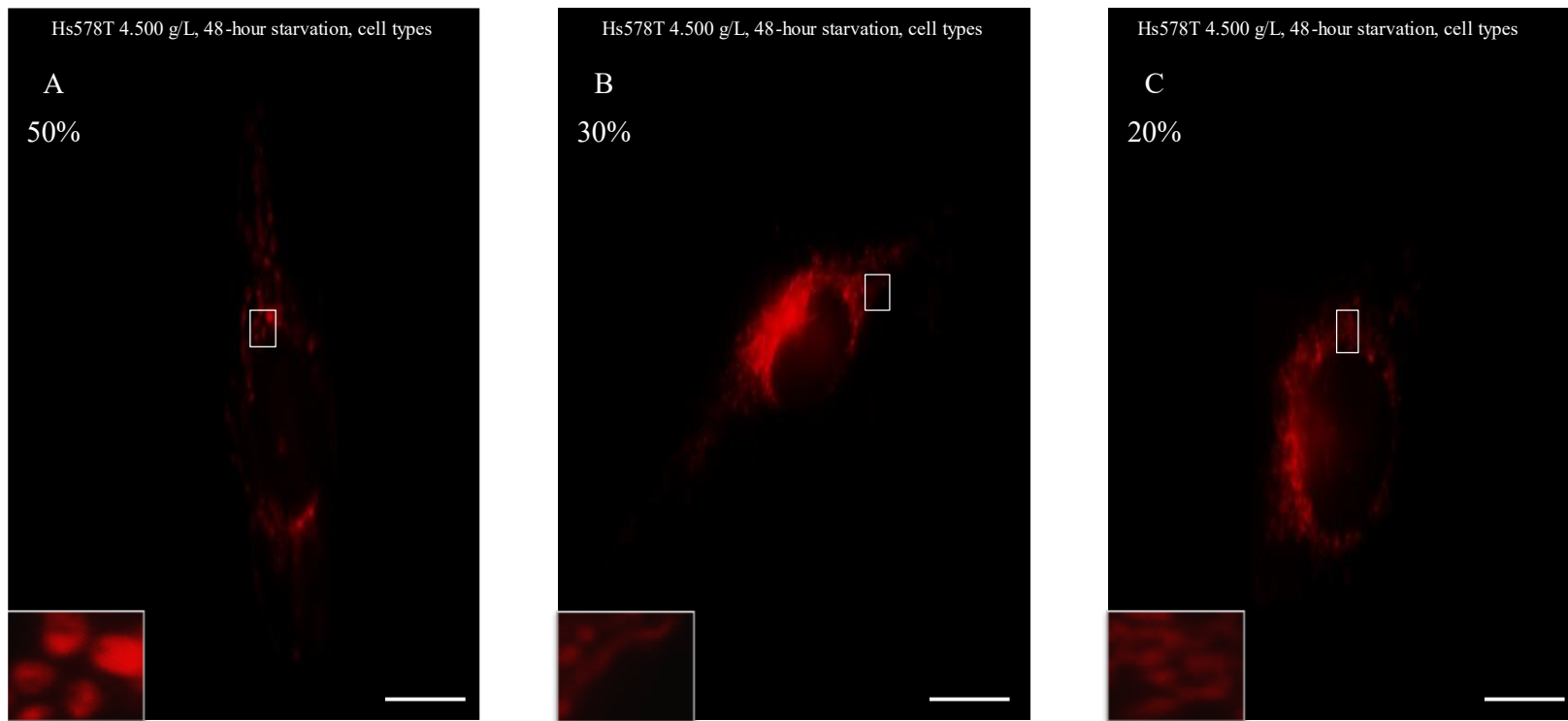


Figure 13. MitoTracker Red Fluorescence staining and imaging of Hs578T cells at 4.500 g/L Representative cell types were chosen to describe the mitochondrial makeup of the entire coverslip seeded with a glucose concentration of 4.500 g/L. Each image was taken at 60X magnification with immersion oil and highlights elongated or shattered mitochondria with their respective frequencies in percentages (A, B, and C).

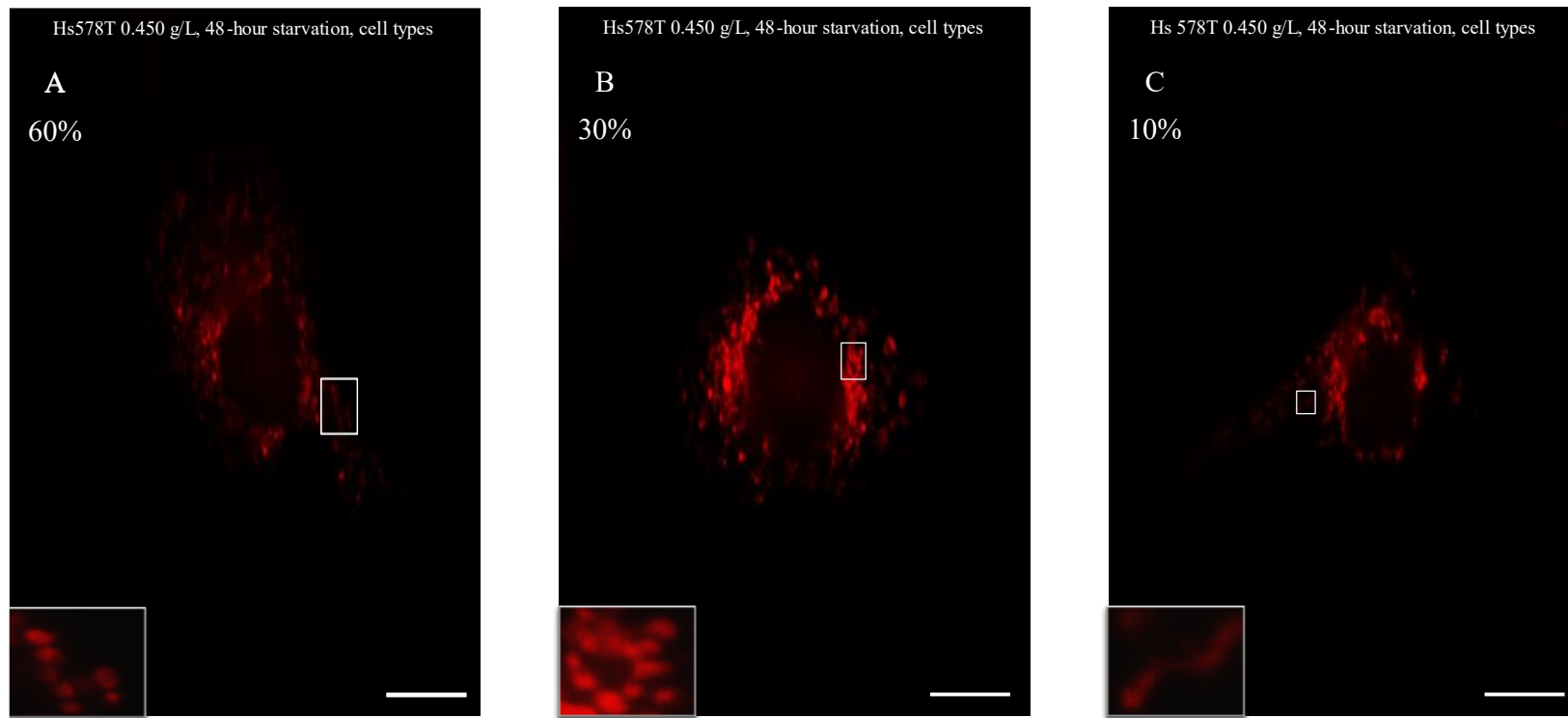


Figure 14. MitoTracker Red Fluorescence staining and imaging of Hs578T cells at 0.450 g/L Representative cell types were chosen to describe the mitochondrial makeup of the entire coverslip seeded with a glucose concentration of 0.450 g/L. Each image was taken at 60X magnification with immersion oil and highlights elongated or shattered mitochondria with their respective frequencies in percentages (A, B, and C)

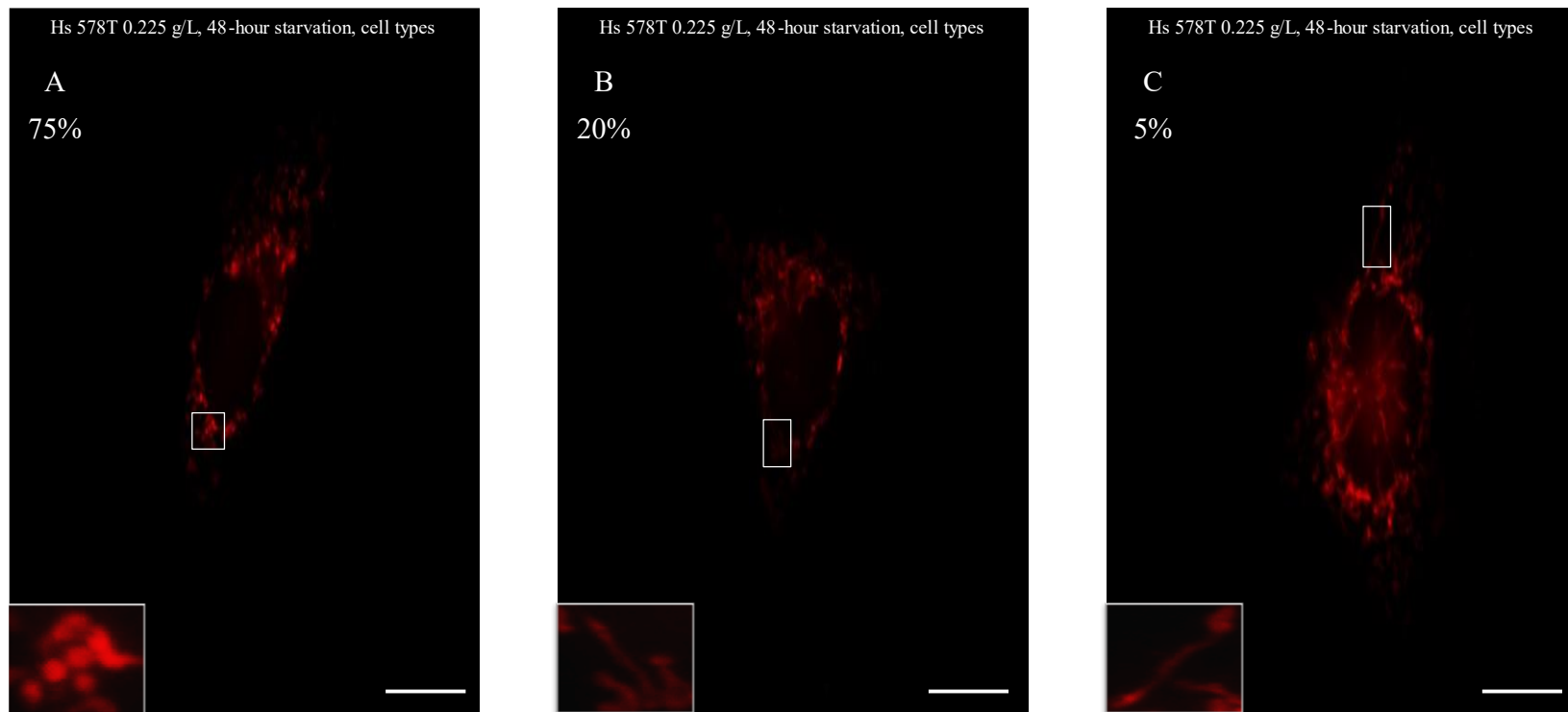


Figure 15. MitoTracker Red Fluorescence staining and imaging of Hs578T cells at 0.225 g/L Representative cell types were chosen to describe the mitochondrial makeup of the entire coverslip seeded with a glucose concentration of 0.225 g/L. Each image was taken at 60X magnification with immersion oil and highlights elongated or shattered mitochondria with their respective frequencies in percentages (A, B, and C).

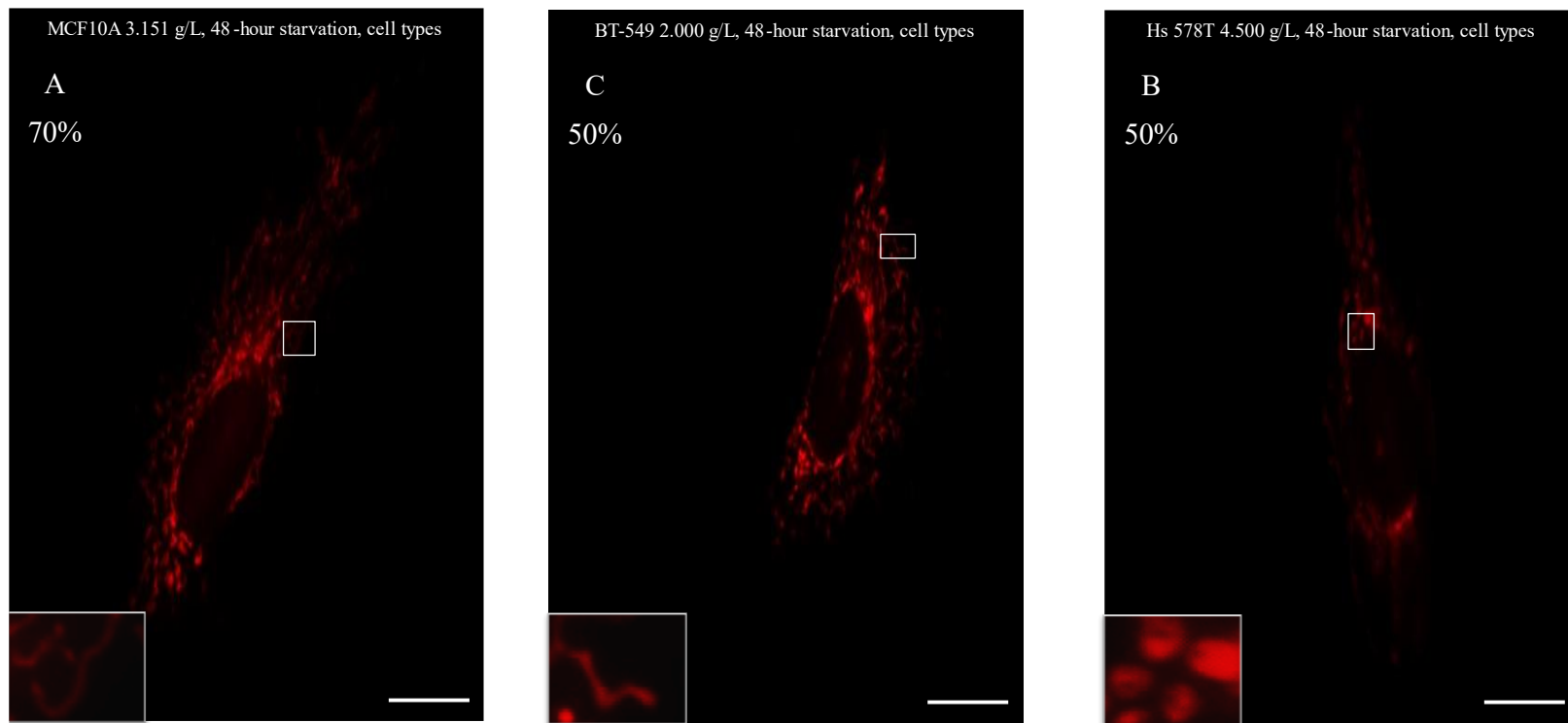


Figure 16. Comparative MitoTracker Red Fluorescence staining and imaging of dominant cell types in their base glucose concentrations Each image represents the most common cell type observed in their base/highest glucose concentration, A (MCF10A at 4.500 g/L), B (BT-549 at 2.000 g/L), and C (Hs 578T at 4.500 g/L), along with an approximation of its overall percentage on their respective slides. Each image was taken at 60X magnification with oil.

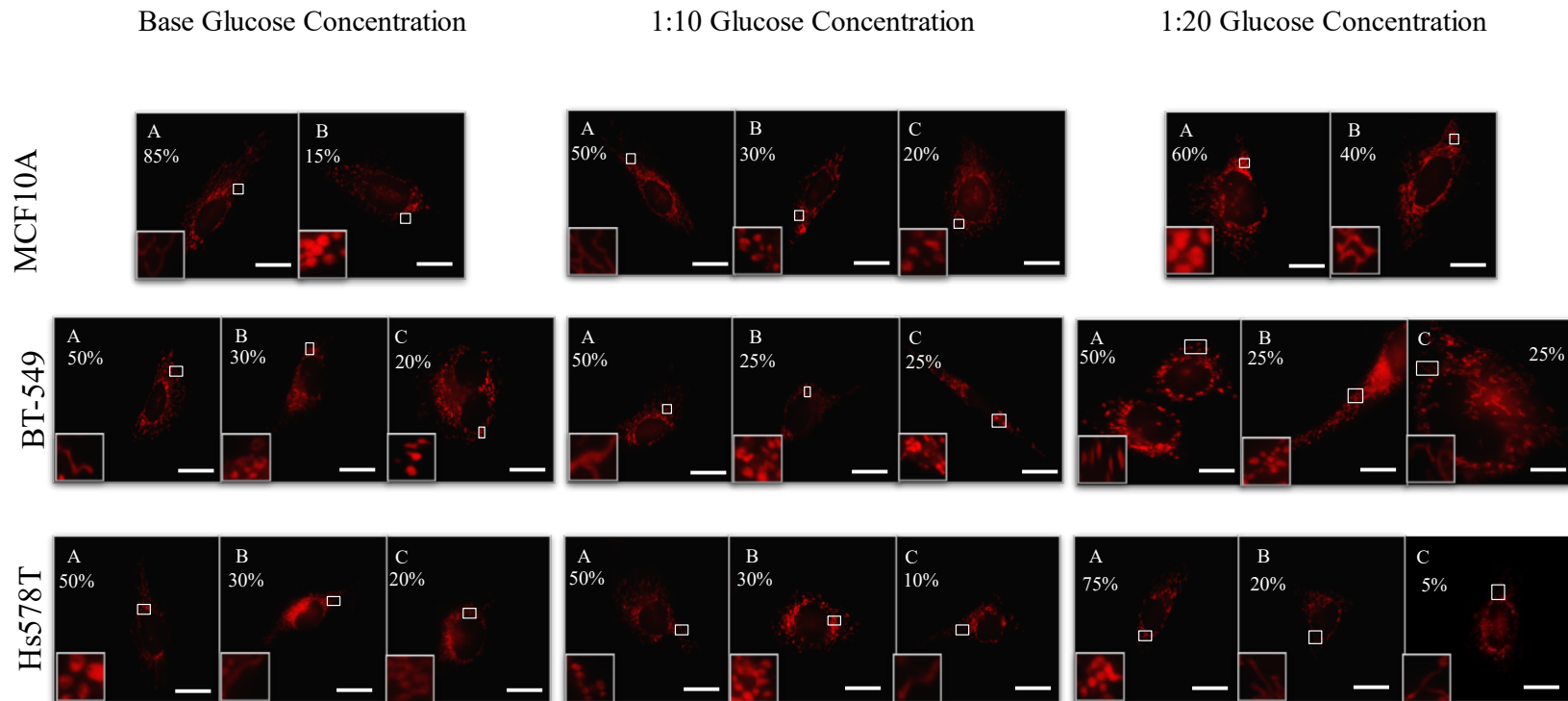


Figure 17. Comparative MitoTracker Red Fluorescence staining and imaging of all three cell lines in all nutrient conditions Images and percentages from each cell line at each glucose condition, Base (left column) 1:10 (middle column), and 1:20 (right column) are placed side-by-side. From the topmost row to bottom most row: MCF10A (top), BT-549 (middle), and Hs578T (bottom).

DISCUSSION

The inconsistencies amongst TNBCs have also provided difficulty to researchers and clinicians due to a lack of reliable markers in comparison to their cousins, luminal and HER2 breast cancers. Yet, heterogeneity in metabolic activity is a defining feature within TNBC. It poses as an interesting target of further study and novel therapeutic approaches. Chemotherapy is amongst first-line options when it comes to treating TNBC. However, effectiveness of chemotherapy on TNBC can be difficult to predict due to the diversity in their biomolecular and metabolic makeups (Emens et al., 2018). Early studies of TNBC have deemed it as a highly glycolytic cancer (Hussein et al., 2011) with aberrant mitochondria (Pelicano et al., 2014). Newer studies with TNBC cells that are resistant to chemotherapy and TNBC cells that have migrated from the original tumor show an increase in OXPHOS activity (Echerverria et al., 2019). DLST and its role within cell maintenance and growth is yet to be fully understood, along with the TCA's role within TNBC. However, discovering TNBC cell line heterogeneity, in respect to DLST expression and dependence, shows a promising biomarker that has influenced this project's direction and objective to understand adaptive properties within TNBC cell lines (Shen et al., 2021).

In this project, we subjected two TNBC cell lines (BT-549 and Hs578T) and one non-tumorigenic epithelial cell line of mammary gland origin (MCF10A) to cellular stress by nutrient starvation to identify if differences in DLST dependence can affect cellular adaptation and regulation of mitochondrial morphology. MCF10A showed the

highest resilience to maintain cell viability amongst all three cell lines and established a consistent, nontumorigenic control for comparison. A shallow decreasing trend was recorded with the largest difference between adjacent columns at approximately 12%. Between the highest glucose concentration and the glucose-free condition, there was an approximate 37% difference in average MCF10A cell viability. When comparing the other glucose concentrations to the control, 4.5000 g/L, MCF10A cells were found to have a significant difference in all concentrations from 0.1406 g/L to the glucose-free condition.

BT-549 showed capacity to maintain high redox activity across a broad spectrum of nutrient stress conditions, showcasing a strong resilience to maintain its redox capabilities like MCF10A. There was a decreasing trend in percentages as the conditions approached the glucose-free condition, noting its largest loss in viability between adjacent columns occurred with an approximate 21% from 0.1406 g/L to 0.0703 g/L. The overall difference in average cell viability between the highest glucose concentration and the glucose-free condition was approximately 47%. In contrast to MCF10A, BT-549 cell viability did show an overall increase in cell viability, but more instances of wider SEM, denoting variability or experimental errors. A deviation from uniformity was observed at 0.2812 g/L, where a significant difference was detected, followed by lower glucose concentrations that did not reach significance until 0.0351 g/L. Potential outlying factors during seeding, incubation, or fluorescence measurements may have influenced cell viability, contributing to greater variability and outliers within the error range. Thus, the

threshold of a significant difference, could potentially start as high as 0.2812 g/L, although it is more likely to occur at a lower concentration.

As glucose concentrations began to wane, MCF10A, BT-549 and Hs578T cells were all able to maintain similar levels of cell viability over 90% until 0.5625 g/L, where Hs578T cells showed the steepest loss in redox potential and average cell viability at approximately 60% between two adjacent concentrations, 0.5625 g/L to 0.2812 g/L. Overall, a decreasing trend in cell viability was also recorded with an approximate 81% decrease between the highest glucose concentration and the glucose-free condition. Hs578T cells were seen to have a significant difference from the control concentration from 0.2812 g/L to the glucose-free concentration.

Overall, MCF10A cells had the highest cell viability percentages at the lower ends of the nutrient spectrum, with smaller recorded drops between adjacent columns and the lowest overall difference in average cell viability percentages between the highest glucose concentration and glucose-free condition. BT-549 cells fell in between that MCF10A and Hs578T, while Hs578T displayed the demonstrated a considerable sensitivity to cellular stress induced by glucose starvation, exhibiting the most pronounced decline in viability amongst all three.

Transitioning to imaging studies, noticeable differences were found in the regulation of mitochondrial structure within TNBC cell lines. MCF10A retained a high frequency of elongated mitochondria. Similarly, BT-549 cells showed high amounts of elongated mitochondria across the glucose concentrations as well. On the other hand, increasing cellular stress in Hs578T cells led to a higher frequency in shattered

mitochondria across all nutrient conditions, showing a higher sensitivity to nutrient stress and a stark difference between the elaborate mitochondrial fusion seen in MCF10A and BT-549.

Combining the data that has been collected about cell viabilities and mitochondrial structures, certain key points become prominent. DLST-dependent BT-549 cells and their metabolic properties are reminiscent to that of MCF10A, as both were able to retain similarly high frequencies of viable cells and elongated mitochondria. Elongated mitochondria contain extensive cristae structure which can save and even increase mitochondrial activity when under cellular stress (Youle et al., 2012) (Gomes et al., 2011). These similarities found in their adaptive potentials exhibits that BT-549 cells remained the property of non-cancerous cells. Oppositely, Hs578T cells had a higher frequency of mitochondria that were physiologically and structurally defunct, establishing its lack of reliance on DLST and altered metabolism that is different to that of MCF10A and BT-549.

Cell viability and fluorescence analysis provides researchers with valuable information to behaviors on a molecular level, but not without their own drawbacks. Cellular metabolism studies are one of many ways to study cell viability. CellTiter-Blue® and other assays that measure redox potential are highly sensitive, effective and cheap. Yet, it indirectly measures for cell viability. Reduce mitochondrial potential is not entirely discriminated from an entire lack of viability (Ghasemi et al., 2021). Combined with the idea that these measurements are not denoting the capabilities of a singular cell but rather a population of cells, fluorescence measurements may not entirely show the

entire image. Though they may be of the same classification, the rate in which certain components of the dye are reduced is not the same amongst all cells within the same well and in adjacent wells, making it difficult to establish an entirely equitable incubation condition (Ghasemi et al., 2021). MitoTracker staining uses a fluorescent probe with lipophilic properties, allowing it to pass the plasma membrane of mitochondria with ease. However, previous studies have shown the challenges to using MitoTracker. The probe specifically targets mitochondria and their ability to maintain mitochondrial membrane potential (Xiao et al., 2016). Our project subjects each cell line to nutrient stress that could lead to potential damage. Though this condition and its effect is sought after in our specific project, there is evidence that shows that mitochondria temporarily lose their membrane potential during the action of fission and fusion (Dong et al., 2022), events that are upregulated under cellular stress. Though MitoTracker is an effective reagent used by many, the representative population of mitochondria within cells is expansive, but not all-encompassing. Mitochondria are also one of many different organelles that have a membrane potential that MitoTracker could be attracted to. Endoplasmic reticulum and lysosomes have a high membrane potential the probe seeks (Klier et al., 2022). This contributed to indiscriminate staining and additional background signal. Despite this, MitoTracker is widely used amongst researchers, and there is room for it to be better understood to ensure that there are no artificial changes to mitochondrial structure as a result of using this probe.

CONCLUSION

The study aimed to understand the adaptive capabilities of TNBC cell lines in respect to their levels of DLST expression. Ultimately, we sought to add to our understanding of DLST and compare the molecular behaviors based on DLST-dependency within TNBC and how it impacts or contributes to cell maintenance and growth in TNBC. First, we identified two TNBC cell lines that would be prime candidates for comparison based off their relative dependency of DLST (Shen et al., 2021). After, we chose two modalities in which we could compare the TNBC cell lines in, cell viability and mitochondrial morphology. MCF10A, BT-549, and Hs578T were then examined after undergoing glucose starvation and cellular stress for 48-hours, mimicking acute conditions that would come from movement cells away from the primary tumor and a change in microenvironment.

Each cell line was measured of their ability to maintain oxidative potential and turn the resazurin in the indicator dye, CellTiter-Blue®, into resorufin. The fluorescent values were recorded and calculated to convey cell viability Hs578T cells were not as capable at adapting to increasing stress conditions, showing lower percent of viable cells at higher glucose levels than the noncancerous control. BT-549 more closely resembled that of MCF10A than that of Hs578T. Higher cell viability percentages were seen in BT-549 across the entire gradient of decreasing glucose concentrations. Imaging studies of the cells stained with MitoTracker™ Red CMXRos, post-starvation period, showed more elaborate and elongated mitochondrial structures in BT-549 and signs of mitochondrial fragmentation in Hs578T. Both cell viability and mitochondrial structure tests confirm

our hypothesis that DLST-dependency correlating to how well the TNBC cell lines can adapt when under cellular stress.

When comparing TNBC cell lines to one another, BT-549's DLST-dependency becomes more apparent when under nutrient stress, especially in fluorescence analysis. This is within our expectations as defined by our previous western blot analysis that showed BT-549 will levels of DLST that are closer to MCF10A and higher than that of Hs578T, and DLST-depletion studies showing affected growth rate in BT-549 and not Hs578T (Shen et al., 2021). In addition, there is room to introduce DLST-depleted TNBC cell lines to the same nutrient stress to compare how the data would differ amongst what was recorded and discussed in this project. The data from this project has acknowledged that DLST and DLST-dependency has value as a predictor of adaptive capabilities and metabolic potential. Furthermore, it supports the notion set by our previous study that DLST has potential as a promising biomarker for TNBC.

The theoretical ceiling for what can come from this project bring light to higher magnification confocal and more effective staining techniques that reduces background signal. 100X imaging would provide a more comprehensive picture to the mitochondria, opening more opportunities for analysis. In this experiment, fluorescent staining has allowed us to see mitochondrial elaboration and mitochondrial fragmentation in respect to comparative, qualitative analysis. However, advancements in super-resolution imaging such as structured illumination microscopy and stimulated emission depletion have allowed for better visualization of mitochondrial elaboration identification of cristae structure. To complement this, open-source machine learning has potential to provide

means to in providing quantitative data such as cristae density and mitochondrial lengths with a high level of precision (Segawa et al., 2020).

For future application, this project establishes quantitative and qualitative metrics that can be used in comparative manners when cell models undergo stress to incite adaptation. Our study design establishes supportive metrics that can be paired with a multitude of other tests to paint a clearer picture of the metabolic activity, biomolecular interactions, and energetic pathways that occur within cells. This can include protein extraction, western blotting, and fluorescent studies that depict ROS production. Pairing other means to measure cell viability, such as those that measure cell growth, would further enhance how understanding of adaptive potentials and simulate metastatic conditions. Additional information such as unbiased metabolomics would allow for us to see what other redox maintaining pathways are affected and how significant the metabolite differences may be. Notably so, the starvation conditions set by this project are best defined as “acute” and “short-term”. Ultimately, this project not only identifies heterogeneity within TNBC cell lines and DLST-dependence but also opens a variety of possibilities in the understanding DLST behavior and its potential as an in-vitro biomarker with translational benefits to be considered within in-vivo and clinical applications.

BIBLIOGRAPHY

- Anderson, N. M., Mucka, P., Kern, J. G., & Feng, H. (2018). The emerging role and targetability of the TCA cycle in cancer metabolism. *Protein & Cell*, 9(2), 216-237. <https://doi.org/10.1007/s13238-017-0451-1>
- Alabduladhem, T. O., & Bordoni, B. (2022). Physiology, Krebs cycle. In *StatPearls* (Updated November 23, 2022). StatPearls Publishing. Retrieved from <https://www.ncbi.nlm.nih.gov/books/NBK556032/>
- Arun, B., Couch, F. J., Abraham, J., et al. (2024). BRCA-mutated breast cancer: The unmet need, challenges, and therapeutic benefits of genetic testing. *British Journal of Cancer*, 131, 1400–1414. <https://doi.org/10.1038/s41416-024-02827-z>
- Asif, H. M., Sultana, S., Ahmed, S., Akhtar, N., & Tariq, M. (2016). HER-2 Positive Breast Cancer - a Mini-Review. *Asian Pacific journal of cancer prevention : APJCP*, 17(4), 1609–1615. <https://doi.org/10.7314/apjcp.2016.17.4.1609>
- Baek, M. L., Lee, J., Pendleton, K. E., Berner, M. J., Goff, E. B., Tan, L., Martinez, S. A., Mahmud, I., Wang, T., Meyer, M. D., Lim, B., Barrish, J. P., Porter, W., Lorenzi, P. L., & Echeverria, G. V. (2023). Mitochondrial structure and function adaptation in residual triple-negative breast cancer cells surviving chemotherapy treatment. *Oncogene*, 42(14), 1117-1131. <https://doi.org/10.1038/s41388-023-02596-8>
- Ban, T., Ishihara, T., Kohno, H., Saita, S., Ichimura, A., Maenaka, K., Oka, T., Mihara, K., & Ishihara, N. (2017). Molecular basis of selective mitochondrial fusion by heterotypic action between OPA1 and cardiolipin. *Nature Cell Biology*, 19, 856–863. <https://doi.org/10.1038/ncb3560>
- Beatson, G. T. (1896). On the treatment of inoperable cases of carcinoma of the mamma: Suggestions for a new method of treatment, with illustrative cases. *Transactions of the Medico-Chirurgical Society of Edinburgh*, 15, 153-179.
- Bedard, P. L., Im, S.-A., Elimova, E., et al. (2022). Zanidatamab (ZW25), a HER2-targeted bispecific antibody, in combination with chemotherapy for HER2-positive breast cancer: Results from a phase 1 study. *Cancer Research*, 82(4 Suppl.), P2-13-07. <https://doi.org/10.1158/1538-7445.SABCS21-P2-13-07>
- Berg, J. M., Tymoczko, J. L., & Stryer, L. (2002). *Biochemistry* (5th ed.). W. H. Freeman.
- Bianchini, G., Balko, J. M., Mayer, I. A., Sanders, M. E., & Gianni, L. (2016). Triple-negative breast cancer: Challenges and opportunities of a heterogeneous disease.

- Nature Reviews Clinical Oncology, 13, 674–690.
<https://doi.org/10.1038/nrclinonc.2016.66>
- Blagov, A. V., Postnov, A. Y., Khotina, V. A., Sukhorukov, V. N., Sadykhov, N. K., & Orekhov, A. N. (2024). The role of mitochondria in metastasis development. *Cellular and molecular biology (Noisy-le-Grand, France)*, 70(1), 171–178.
<https://doi.org/10.14715/cmb/2024.70.1.23>
- Brock, A. H., Zhang, A., Buschhaus, J. M., Bevoor, A., Farfel, A., Rajendran, S., Cutter, A. C., & Luker, G. D. (2023). Enhanced mitochondrial fission inhibits triple-negative breast cancer cell migration through an ROS-dependent mechanism. *iScience*, 26(6), 106788. <https://doi.org/10.1016/j.isci.2023.106788>
- Cardaci, S., & Ciriolo, M. R. (2012). TCA cycle defects and cancer: When metabolism tunes redox state. *International Journal of Cell Biology*, 2012, 161837.
<https://doi.org/10.1155/2012/161837>
- Chan, D. C. (2020). Mitochondrial dynamics and its involvement in disease. *Annual Review of Pathology: Mechanisms of Disease*, 15, 235-259.
<https://doi.org/10.1146/annurev-pathmechdis-012419-032711>
- Cogliati, S., Frezza, C., Soriano, M. E., Varanita, T., Quintana-Cabrera, R., Corrado, M., Cipolat, S., Costa, V., Casarin, A., Gomes, L. C., Perales-Clemente, E., Salviati, L., Fernandez-Silva, P., Enriquez, J. A., & Scorrano, L. (2013). Mitochondrial cristae shape determines respiratory chain supercomplexes assembly and respiratory efficiency. *Cell*, 155(1), 160-171. <https://doi.org/10.1016/j.cell.2013.08.032>
- Echeverria, G. V., Ge, Z., Seth, S., Zhang, X., Jeter-Jones, S., Zhou, X., Cai, S., Tu, Y., McCoy, A., Peoples, M., Sun, Y., Qiu, H., Chang, Q., Bristow, C., Carugo, A., Shao, J., Ma, X., Harris, A., Mundi, P., ... Piwnica-Worms, H. (2019). Resistance to neoadjuvant chemotherapy in triple-negative breast cancer mediated by a reversible drug-tolerant state. *Science Translational Medicine*, 11(488), eaav0936.
<https://doi.org/10.1126/scitranslmed.aav0936>
- Emens, L. A. (2018). Breast cancer immunotherapy: Facts and hopes. *Clinical Cancer Research*, 24(3), 511-520. <https://doi.org/10.1158/1078-0432.CCR-16-3001>
- Evans, K. W., Yuca, E., Scott, S. S., Zhao, M., Paez Arango, N., Cruz Pico, C. X., Saridogan, T., Shariati, M., Class, C. A., Bristow, C. A., Vellano, C. P., Zheng, X., Gonzalez-Angulo, A. M., Su, X., Tapia, C., Chen, K., Akcakanat, A., Lim, B., Tripathy, D., ... Meric-Bernstam, F. (2021). Oxidative phosphorylation is a metabolic vulnerability in chemotherapy-resistant triple-negative breast cancer. *Cancer Research*, 81(21), 5572-5581. <https://doi.org/10.1158/0008-5472.CAN-20-3242>

- Giaquinto, A. N., Sung, H., Newman, L. A., Freedman, R. A., Smith, R. A., Star, J., Jemal, A., & Siegel, R. L. (2024). Breast cancer statistics 2024. *CA: A Cancer Journal for Clinicians*, 74(6), 477-495. <https://doi.org/10.3322/caac.21863>
- Ghasemi, M., Turnbull, T., Sebastian, S., & Kempson, I. (2021). The MTT Assay: Utility, Limitations, Pitfalls, and Interpretation in Bulk and Single-Cell Analysis. *International journal of molecular sciences*, 22(23), 12827. <https://doi.org/10.3390/ijms222312827>
- Gloeckner, H., Jonuleit, T., & Lemke, H. D. (2001). Monitoring of cell viability and cell growth in a hollow-fiber bioreactor by use of the dye Alamar Blue. *Journal of Immunological Methods*, 252, 131–138.
- Goldner, M., Pandolfi, N., Maciel, D., Lima, J., Sanches, S., & Pondé, N. (2021). Combined endocrine and targeted therapy in luminal breast cancer. *Expert Review of Anticancer Therapy*, 21(11), 1237-1251. <https://doi.org/10.1080/14737140.2021.1960160>
- Hussein, Y. R., Bandyopadhyay, S., Semaan, A., Ahmed, Q., Albashiti, B., Jazaerly, T., Nahleh, Z., & Ali-Fehmi, R. (2011). Glut-1 expression correlates with basal-like breast cancer. *Translational Oncology*, 4(6), 321-327. <https://doi.org/10.1593/tlo.11256>
- Imbalzano, K. M., Tatarkova, I., Imbalzano, A. N., & Nickerson, J. A. (2009). Increasingly transformed MCF-10A cells have a progressively tumor-like phenotype in three-dimensional basement membrane culture. *Cancer Cell International*, 9(7). <https://doi.org/10.1186/1475-2867-9-7>
- Inic, Z., Zegarac, M., Inic, M., Markovic, I., Kozomara, Z., Djuricic, I., Inic, I., Pupic, G., & Jancic, S. (2014). Difference between Luminal A and Luminal B subtypes according to Ki-67, tumor size, and progesterone receptor negativity providing prognostic information. *Clinical Medicine Insights: Oncology*, 8, 107–111. <https://doi.org/10.4137/CMO.S18006>
- Iqbal, N., & Iqbal, N. (2014). Human epidermal growth factor receptor 2 (HER2) in cancers: Overexpression and therapeutic implications. *Molecular Biology International*, 2014, 852748. <https://doi.org/10.1155/2014/852748>
- Karim, A. M., Eun Kwon, J., Ali, T., Jang, J., Ullah, I., Lee, Y. G., Park, D. W., Park, J., Jeang, J. W., & Kang, S. C. (2023). Triple-negative breast cancer: epidemiology, molecular mechanisms, and modern vaccine-based treatment strategies. *Biochemical pharmacology*, 212, 115545. <https://doi.org/10.1016/j.bcp.2023.115545>

- Kim, D., & Nam, H. J. (2022). PARP inhibitors: Clinical limitations and recent attempts to overcome them. *International Journal of Molecular Sciences*, 23(15), 8412. <https://doi.org/10.3390/ijms23158412>
- Klier, P. E., Roo, R., & Miller, E. W. (2022). Fluorescent indicators for imaging membrane potential of organelles. *Current opinion in chemical biology*, 71, 102203.
- Mansoury, M., Hamed, M., Karmustaji, R., Al Hannan, F., & Safrany, S. T. (2021). The edge effect: A global problem. The trouble with culturing cells in 96-well plates. *Biochemistry and Biophysics Reports*, 26, 100987. <https://doi.org/10.1016/j.bbrep.2021.100987>
- Massagué, J., & Obenauf, A. C. (2016). Metastatic colonization by circulating tumour cells. *Nature*, 529(7586), 298–306. <https://doi.org/10.1038/nature17038>
- McBride, H., & Soubannier, V. (2010). Mitochondrial function: OMA1 and OPA1, the grandmasters of mitochondrial health. *Current Biology*, 20(R274–R276). <https://doi.org/10.1016/j.cub.2010.02.011>
- Merkwirth, C., Dargazanli, S., Tatsuta, T., Geimer, S., Löwer, B., Wunderlich, F. T., von Kleist-Retzow, J. C., Waisman, A., Westermann, B., & Langer, T. (2008). Prohibitins control cell proliferation and apoptosis by regulating OPA1-dependent cristae morphogenesis in mitochondria. *Genes & Development*, 22(4), 476–488. <https://doi.org/10.1101/gad.460708>
- Merkwirth, C., & Langer, T. (2009). Prohibitin function within mitochondria: Essential roles for cell proliferation and cristae morphogenesis. *Biochimica et Biophysica Acta (BBA) - Molecular Cell Research*, 1793, 27–32. <https://doi.org/10.1016/j.bbamcr.2008.05.013>
- Miah, S., Bagu, E., & Goel, R. (2019). Estrogen receptor signaling regulates the expression of the breast tumor kinase in breast cancer cells. *BMC Cancer*, 19, 78. <https://doi.org/10.1186/s12885-018-5186-8>
- Neikirk, K., Marshall, A., Kula, B., Smith, N., LeBlanc, S., & Hinton, A. (2023). MitoTracker: A useful tool in need of better alternatives. *European Journal of Cell Biology*, 102(4), 151371. <https://doi.org/10.1016/j.ejcb.2023.151371>
- Nielsen, T. O., Hsu, F. D., Jensen, K., Cheang, M., Karaca, G., Hu, Z., Hernandez-Boussard, T., Livasy, C., Cowan, D., Dressler, L., Akslen, L. A., Ragaz, J., Gown, A. M., Gilks, C. B., van de Rijn, M., & Perou, C. M. (2004). Immunohistochemical and clinical characterization of the basal-like subtype of invasive breast carcinoma. *Clinical Cancer Research*, 10(16), 5367–5374. <https://doi.org/10.1158/1078-0432.CCR-04-0220>

- Olichon, A., Emorine, L. J., Descoins, E., Pelloquin, L., Bricchese, L., Gas, N., Guillou, E., Delettre, C., Valette, A., Hamel, C. P., Ducommun, B., Lenaers, G., & Belenguer, P. (2002). The human dynamin-related protein OPA1 is anchored to the mitochondrial inner membrane facing the inter-membrane space. *FEBS Letters*, 523(1–3), 171–176. [https://doi.org/10.1016/s0014-5793\(02\)02985-x](https://doi.org/10.1016/s0014-5793(02)02985-x)
- Orrantia-Borunda, E., Anchondo-Nuñez, P., Acuña-Aguilar, L. E., et al. (2022). Subtypes of breast cancer. In H. N. Mayrovitz (Ed.), *Breast cancer*. Exon Publications. <https://doi.org/10.36255/exon-publications-breast-cancer-subtypes>
- Ward, P. S., & Thompson, C. B. (2012). Metabolic reprogramming: A cancer hallmark even Warburg did not anticipate. *Cancer Cell*, 21(3), 297–308. <https://doi.org/10.1016/j.ccr.2012.02.014>
- Pelicano, H., Zhang, W., Liu, J., Hammoudi, N., Dai, J., Xu, R. H., Pusztai, L., & Huang, P. (2014). Mitochondrial dysfunction in some triple-negative breast cancer cell lines: Role of mTOR pathway and therapeutic potential. *Breast Cancer Research*, 16(5), 434. <https://doi.org/10.1186/s13058-014-0434-6>
- Rashid, M. U., & Coombs, K. M. (2019). Serum-reduced media impacts on cell viability and protein expression in human lung epithelial cells. *Journal of Cellular Physiology*, 234(6), 7718–7724. <https://doi.org/10.1002/jcp.27890>
- Robinson, B. H., Petrova-Benedict, R., Buncic, J. R., & Wallace, D. C. (1992). Nonviability of cells with oxidative defects in galactose medium: A screening test for affected patient fibroblasts. *Biochemical Medicine and Metabolic Biology*, 48, 122–126. [https://doi.org/10.1016/0885-4505\(92\)90056-5](https://doi.org/10.1016/0885-4505(92)90056-5)
- Schnyder, S. K., Molina, J. J., & Yamamoto, R. (2020). Control of cell colony growth by contact inhibition. *Scientific Reports*, 10, 6713. <https://doi.org/10.1038/s41598-020-62913-z> Segawa M, Wolf DM, Hultgren NW, Williams DS, van der Blik AM, Shackelford DB, Liesa M, Shirihai OS. Quantification of cristae architecture reveals time-dependent characteristics of individual mitochondria. *Life Sci Alliance*. 2020 Jun 4;3(7):e201900620. doi: 10.26508/lsa.201900620. PMID: 32499316; PMCID: PMC7283135.
- Sendur, M. A., Aksoy, S., & Altundag, K. (2013). Cardiotoxicity of novel HER2-targeted therapies. *Current Medical Research and Opinion*, 29(8), 1015–1024. <https://doi.org/10.1185/03007995.2013.807232>
- Shen, N., Korm, S., Karantanos, T., et al. (2021). DLST-dependence dictates metabolic heterogeneity in TCA-cycle usage among triple-negative breast cancer. *Communications Biology*, 4, 1289. <https://doi.org/10.1038/s42003-021-02805-8>

- Sheng, Z. H. (2014). Mitochondrial trafficking and anchoring in neurons: New insight and implications. *Journal of Cell Biology*, 204(7), 1087–1098. <https://doi.org/10.1083/jcb.201312123>
- Shields, H. J., Traa, A., & Van Raamsdonk, J. M. (2021). Beneficial and detrimental effects of reactive oxygen species on lifespan: A comprehensive review of comparative and experimental studies. *Frontiers in Cell and Developmental Biology*, 9, 628157. <https://doi.org/10.3389/fcell.2021.628157>
- Signorile, A., Sgaramella, G., Bellomo, F., & De Rasmio, D. (2019). Prohibitins: A critical role in mitochondrial functions and implication in diseases. *Cells*, 8(1), 71. <https://doi.org/10.3390/cells8010071>
- Steglich, G., Neupert, W., & Langer, T. (1999). Prohibitins regulate membrane protein degradation by the m-AAA protease in mitochondria. *Molecular and Cellular Biology*, 19(5), 3435–3442. <https://doi.org/10.1128/MCB.19.5.3435>
- Takaoka, M., & Miki, Y. (2018). BRCA1 gene: Function and deficiency. *International Journal of Clinical Oncology*, 23(1), 36–44. <https://doi.org/10.1007/s10147-017-1182-2>
- Trefely, S., Lovell, D., Snyder, N., & Wellen, K. (2020). Compartmentalised acyl-CoA metabolism and roles in chromatin regulation. *Molecular Metabolism*, 38, 100941. <https://doi.org/10.1016/j.molmet.2020.01.005>
- Verma, S., Miles, D., Gianni, L., Krop, I. E., Welslau, M., Baselga, J., Pegram, M., Oh, D. Y., Diéras, V., Guardino, E., Fang, L., Lu, M. W., Olsen, S., Blackwell, K., & EMILIA Study Group. (2012). Trastuzumab emtansine for HER2-positive advanced breast cancer. *New England Journal of Medicine*, 367(19), 1783–1791. <https://doi.org/10.1056/NEJMoa1209124>
- Westrate, L. M., Drocco, J. A., Martin, K. R., Hlavacek, W. S., & MacKeigan, J. P. (2014). Mitochondrial morphological features are associated with fission and fusion events. *PLoS ONE*, 9(4), e95265. <https://doi.org/10.1371/journal.pone.0095265>
- Xiao, B., Deng, X., Zhou, W., & Tan, E. K. (2016). Flow cytometry-based assessment of mitophagy using MitoTracker. *Frontiers in Cellular Neuroscience*, 10, 76. <https://doi.org/10.3389/fncel.2016.00076>
- Youle, R. J., & van der Bliek, A. M. (2012). Mitochondrial fission, fusion, and stress. *Science*, 337(6098), 1062–1065. <https://doi.org/10.1126/science.1219855>

Zaha, D. C. (2014). Significance of immunohistochemistry in breast cancer. *World Journal of Clinical Oncology*, 5(3), 382–392. <https://doi.org/10.5306/wjco.v5.i3.382>

Zeidler, J. D., Fernandes-Siqueira, L. O., Carvalho, A. S., Cararo-Lopes, E., Dias, M. H., Ketzer, L. A., Galina, A., & Da Poian, A. T. (2017). Short-term starvation is a strategy to unravel the cellular capacity of oxidizing specific exogenous/endogenous substrates in mitochondria. *Journal of Biological Chemistry*, 292(34), 14176–14187. <https://doi.org/10.1074/jbc.M117.786582>

Zhang, M. H., Man, H. T., Zhao, X. D., Dong, N., & Ma, S. L. (2013). Estrogen receptor-positive breast cancer molecular signatures and therapeutic potentials (Review). *Biomedical Reports*, 2(1), 41–52. <https://doi.org/10.3892/br.2013.187>

Zick, M., Rabl, R., & Reichert, A. S. (2009). Cristae formation-linking ultrastructure and function of mitochondria. *Biochimica et biophysica acta*, 1793(1), 5–19. <https://doi.org/10.1016/j.bbamcr.2008.06.013>

CURRICULUM VITAE

